Parametric optimisation of methanol combustion in marine dual-fuel engines at low loads

Karvounis, Panagiotis; Theotokatos, Gerasimos; Zoumpourlos, Konstantinos; Coraddu, Andrea

DOI
10.1016/j.applthermaleng.2025.128652

Publication date
2025

Document Version
Final published version

Published in
Applied Thermal Engineering

Applied Thermal Engineering 281 (2025) 128652

Contents lists available at ScienceDirect

Applied Thermal Engineering

journal homepage: www.elsevier.com/locate/apthermeng

Research Paper

Parametric optimisation of methanol combustion in marine dual-fuel engines at low loads

Panagiotis Karvounis [a,*], Gerasimos Theotokatos [a], Konstantinos Zoumpourlos [b], Andrea Coraddu [b]

[a] Maritime Safety Research Centre, Department of Naval Architecture, Ocean, and Marine Engineering, University of Strathclyde, Glasgow G4 0LZ, United Kingdom
[b] Department of Maritime and Transport Technology, Delft University of Technology, Delft 2628 CD, the Netherlands

ARTICLE INFO

Keywords:
Marine dual fuel engine
Methanol
Low loads operation
Multi-injection
Stratified injection
Parametric optimisation
CFD

ABSTRACT

Methanol is considered an alternative fuel for the shipping decarbonisation, the properties of which, however, impact the marine dual-fuel engines ignition and combustion characteristics, especially at low load conditions. This study aims at parametrically optimising a marine dual-fuel engine operating with methanol high energy fraction at low loads to achieve knock-free combustion with the highest efficiency and lowest emissions. Computational Fluid Dynamics (CFD) modelling in the CONVERGE software is employed for the investigated large-bore marine four stroke engine considering four injection strategies including single, two stage and stratified injection. The Reynolds Averaged Navier Stokes (RANS) approach is employed to represent turbulence, the Lagrangian-Eulerian approach is used for the spray formation, and the SAGE detailed chemistry solver is used for modelling combustion. The CFD model was first developed and validated for the engine diesel mode. Subsequently, the validated model was expanded to accommodate the direct injection (DI) of both methanol and diesel fuels. Parametric runs are performed considering the compression ratio (CR) in the range 14–17 and the temperature range at inlet valve closing (T_{IVC}) 360–400 K. The results reveal that acceptable combustion efficiency and high thermal efficiency are achieved with CR and T_{IVC} above 17 and 380 K respectively for single injection, above 16 and 380 K respectively for double injection, as well as above 14 and 360 K respectively for stratified injection. Stratified injection is proposed to improve engine performance and reduce NOx emissions. This study provides insights to achieve stable and efficient operation of methanol-fuelled marine engines at low loads, and as such it contributes to the maritime industry decarbonisation.

1. Introduction

Methanol has attracted interest as a potential fuel to achieve shipping decarbonisation, due to its production scalability, physicochemical characteristics [1–3], and storage requirements [4]. However, methanol adoption in marine engines faces challenges pertaining to its high autoignition temperature compared to diesel [5], methanol lower energy density (associated with higher fuel consumption and considerable shipboard storage space) [6], and safety due to its toxicity [7].

To overcome the autoignition limitations, methanol is mostly used in dual-fuel engines with diesel being the pilot fuel. Compared to diesel, methanol has significantly higher laminar flame velocity, which causes combustion instabilities such as roar and knocking [8]. For methanol port injection engines, the formed in-cylinder homogenous methanol–air mixture results in intensified knocking [9,10], hence limiting the diesel substitution energy ratio to 40–60 % [11,12]. Methanol direct injection (DI), where both methanol and diesel are injected in-cylinder at different timings, allows for higher diesel substitution ratios, as the methanol diffusive combustion exhibits lower knocking tendency [13]. Due to lower in-cylinder temperature attributed to the methanol high latent heat of vaporisation and increased methanol mass to achieve the same energy input compared to diesel, NOx emissions are significantly reduced for both methanol port and direct injection engines [14,15]. The cooling effect from methanol evaporation results to reduced compression work and higher thermal efficiency [16].

Methanol latent heat of vaporisation and cetane number affects the in-cylinder phenomena in contradicting ways. The former leads to reduced in-cylinder temperature, as well as lower values of maximum pressure and peak heat release [17], while the latter increases the ignition delay and, therefore, contributes to knock [18]. These

* Corresponding author.
E-mail address: panagiotis.karvounis@strath.ac.uk (P. Karvounis).

https://doi.org/10.1016/j.applthermaleng.2025.128652
Received 2 July 2025; Received in revised form 16 September 2025; Accepted 6 October 2025
Available online 11 October 2025

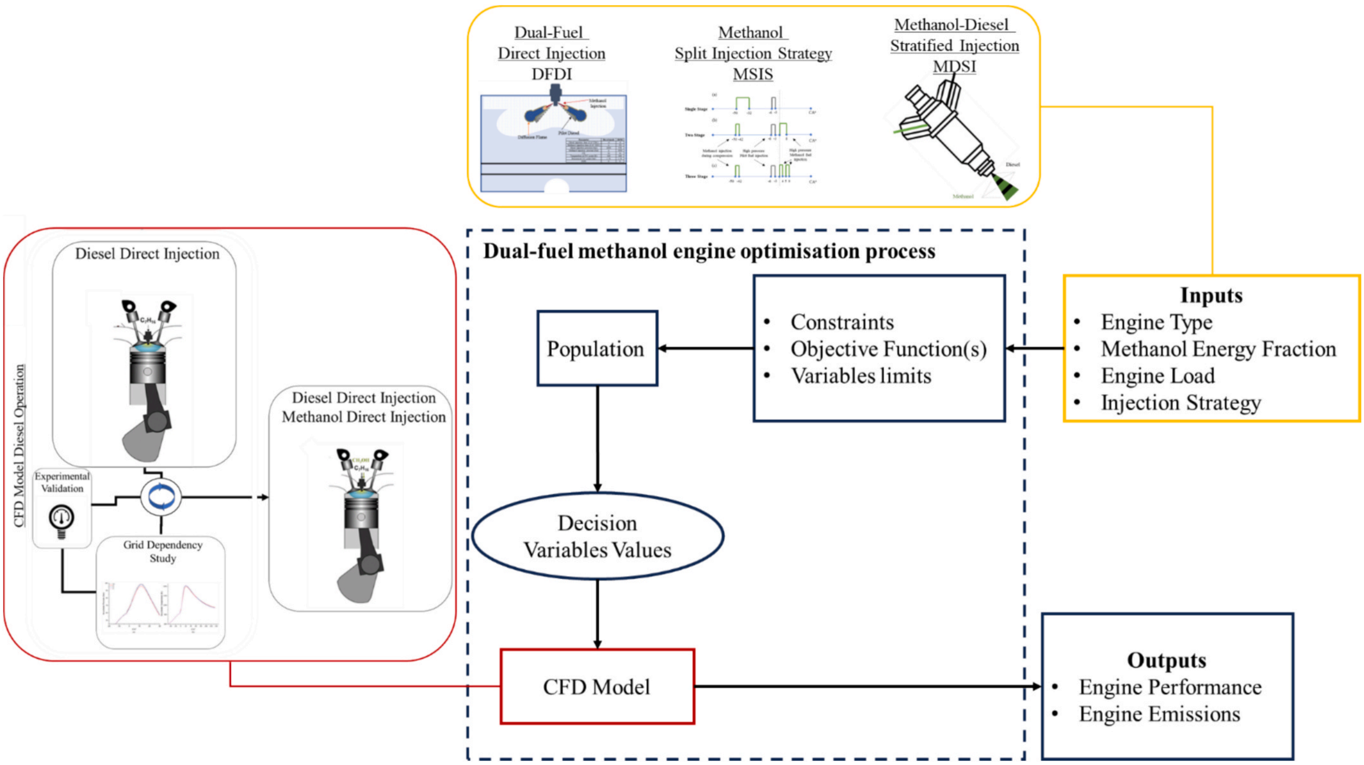

Fig. 1. Dual-fuel engine optimisation methodology flowchart.

conditions depend on the in-cylinder reactivity, and hence, high methanol shares results in increased ringing intensity [8] at medium and high loads, requiring appropriate mitigation measures [19]. On the contrary, at low loads, where the in-cylinder reactivity is reduced, pilot diesel injection may not be adequate to initiate combustion [20]. Therefore, operation in low loads requires measures to overcome the limitation of low combustion efficiency [21].

The intake temperature increase is proposed as a potential mitigation measure to increase the in-cylinder reactivity and facilitate stable methanol combustion. Zincir et al. [22] reported that the intake temperature increase from 102 °C to 107 °C resulted in reducing the ignition delay and combustion efficiency improvement. Furthermore, increasing the compression ratio also improves the in-cylinder reactivity [20]. Valera et al. [23] argued that methanol injection in high temperature improves its atomisation. Kumar et al. [24] reported that increased intake temperature is essential for effective energy conversion. Both increase in intake temperature and compression ratio result in NOx emissions increase. The latter was also reported by Zhang et al. [25] for an engine operating in low loads for an intelligent charge compression ignition combustion method with several injection strategies leading to low temperature combustion. Garcia et al. [26] reported that at low load and speed operation, glow plugs and increased intake temperature are not adequate to address inefficient combustion (with combustion efficiency being less than 92 %).

The injection strategy and in-cylinder initial conditions impact the methanol combustion and emissions [27]. Huang et al. [28] proposed a split injection strategy in a methanol-diesel dual fuel engine for 50 % diesel substitution, which effectively reduced CO, NOx and HC emissions. Li et al. [29] recommended 5 % increase of the temperature at inlet valve close to improve the combustion efficiency for an engine operating with direct dual fuel injection, 70 % methanol share in low loads.

A double injection strategy can potentially reduce the requirement for increased intake temperature [30]. Other strategies may include the use of cetane improvers that are expected to increase the methanol ignitability, reducing the need for multi-injection strategies, and/or increased compression ratio and intake temperatures [31]. For marine engines, significant amount of ignition enhancer is required, whereas potential safety issues must also be addressed. Since diesel and methanol are immiscible liquids, it is possible to achieve methanol-diesel stratified injection, which results in reduced NOx and PM emissions [32,33]. Jia et al. [34] reported that diesel-methanol stratified injection resulted in lower emissions compared to reactivity control compression ignition, which was also supported by Huag at al. [35] for a light duty diesel engine.

The preceding literature review identified the following research gaps: (a) studies dealing with marine dual fuel direct injection engines operating with high methanol fractions in low loads are limited; (b) the methanol injection strategies impact on marine engines performance and emissions is not quantified; (c) two-stage and three-stage injection as well as stratified methanol-diesel injection strategies for marine engines with high methanol fractions in low loads are not investigated.

This study aims at parametrically optimising a marine dual-fuel engine settings operating with 90 % methanol energy fraction in low loads considering different injection strategies, namely single, double, triple, and stratified injection. For each injection strategy, the optimal values/ranges of the compression ratio (CR), and temperature at the inlet valve closing are determined to achieve combustion efficiency greater than 97 %. The trade-offs between indicated thermal efficiency and NOx emissions are also identified. This study focuses on low-loads, as the air–fuel mixture reactivity is reduced due to the charge low temperature and low methanol cetane number.

The novelty of the study stems from: (a) quantification of the effects of the intake temperature and compression ratio on the combustion efficiency in low loads operation (of methanol-diesel dual-fuel marine engine); (b) comparative assessment of the single, double, and triple, and stratified injection strategies and quantification on their effects on combustion and emissions parameters; (c) identification of the trade-offs between combustion and thermal efficiency and NOx emissions for the considered injection strategies and several operating conditions.

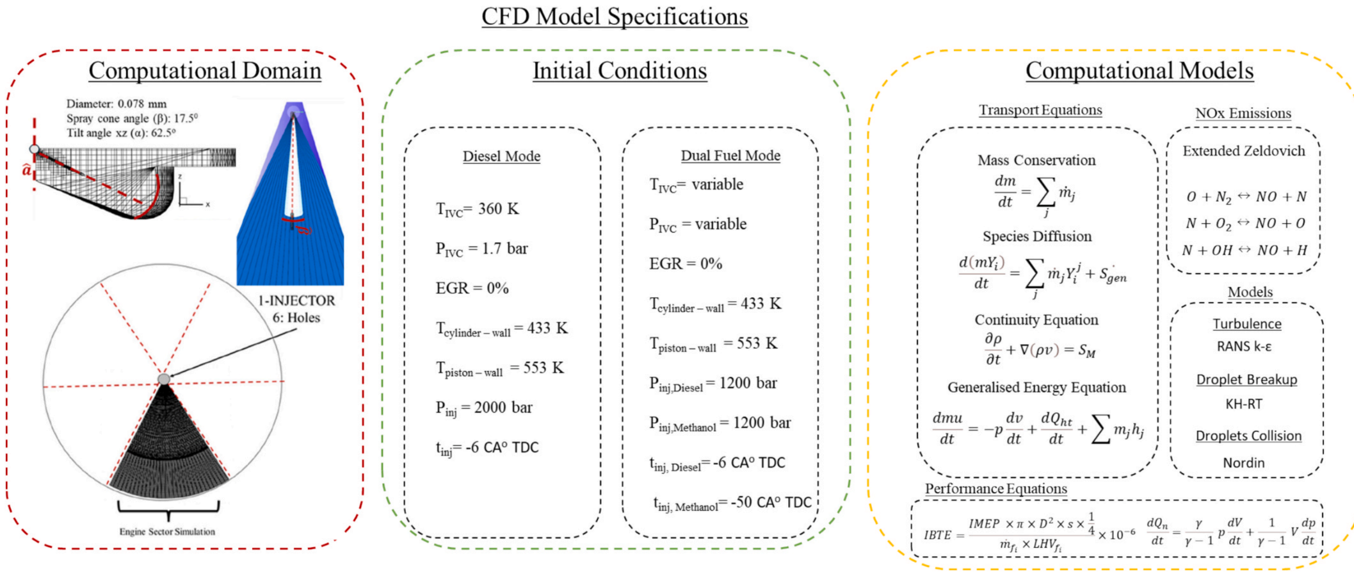

Fig. 2. Employed computational domain, initial conditions and models.

The study provides insights on identifying effective methanol injection strategies for marine dual fuel engines at low loads, and generates information required for future optimisation studies.

2. Methodology

The methodology illustrated in the flowchart of Fig. 1 is employed to perform the parametric optimisation of the investigated marine dual-fuel engine. The inputs include the engine type, methanol energy fraction, engine load and injection strategies. Based on the input and the variables ranges, the initial population is generated. Subsequently, according to the decision variable values and the provided input parameters, the CFD model determines the engine performance, emissions. The CFD model consists of an engine cylinder and is developed in the CONVERGE-CFD software for the diesel mode, as well as the dual-fuel mode with methanol direct injection. The developed models are validated against available measured data for a marine diesel engine and a light-duty dual-fuel engine operating with methanol. Subsequently, a grid sensitivity study is performed to select the grid parameters compromising between acceptable accuracy and required computational effort. For each injection strategy, parametric runs are performed for the determined ranges of the compression ratio and temperature at inlet valve closing. The simulation results are analysed to appraise the engine performance and emissions parameters considering the combustion efficiency, indicated thermal efficiency, and NOx emissions, leading to the determination of optimal values/ranges for the engine settings.

The optimisation objectives include the engine indicated thermal efficiency (Eq. (1)), the NOx emissions and the unburnt methanol emissions. The optimisation constraint is to achieve combustion efficiency above 97 % [36], according to Eq. (2).

$$\eta_{th} = \frac{\int_{IVC}^{EVO} pdV}{Q_{in}} \tag{1}$$

$$\eta_{c,M} = \frac{\int_{IVC}^{EVO} HRR\, dCA}{Q_{in}} > 0.97 \tag{2}$$

where, Q_{in} is the input fuel energy, p is the in-cylinder pressure, V is the cylinder volume and HRR is the heat release rate.

The parametric optimisation is performed for each injection method. Table 2 lists the considered optimisation variables, which are classified in two groups (A and B). This study focuses on Group A and considers the direct injection of both fuels. The pertinent literature review argues that the boost pressure exhibits limited effects on the combustion efficiency and hence this parameter is not used in the optimisation process. The considered injection strategies and variables ranges are discussed in the subsequent paragraphs. The investigation of optimisation variables from Group B is left for future studies.

2.1. CFD model

Fig. 2 provides information on the computational domain, the initial conditions and the employed models. Due to the cylinder symmetry, a sector is selected as the domain of the investigated engine to reduce the computational time. For the diesel mode, the initial values for the temperature and pressure at the inlet valve closing were set to 360 K and 1.7 bar respectively. The injection pressure of the diesel fuel is 1200 bar. For the DFDI mode, it was assumed that these initial parameters vary within selected ranges. Both fuels are injected from the same injector at different timings in order to facilitate split injection strategies. The methanol injection starts at 50 °CA BTDC to enable adequate mixing with the charge air, which benefits ignition and emissions [37]. The methanol injection pressure is set 1,000 bar to facilitate improved atomisation and hence, reduced NOx emissions [19].

The developed CFD models employ the mass conservation, diffusion species, continuity, and generalised energy equations. The extended Zeldovich model is employed to estimate the NOx emissions [38]. The model does not consider prompt NOx creation that constitute a small fraction of thermal NOx especially in dual-fuel combustion with high methanol fraction [39]. The Reynolds Averaged Navier Stokes (RANS) k-ε [40], and KH-RT [41] models are used for the calculation of turbulence and droplet breakup, respectively. The detailed Andrae and Head reaction mechanism is employed, which with considers 672 reactions and 143 species [42]. The developed models particulars are listed in Table A1 (Appendix).

This study considers the following assumptions: (1) the injection pressure, timings and nozzle geometrical characteristics remain constant for the examined cases; (2) the working medium is considered ideal gas; (3) trapezoidal injection pulses are considered for the direct injection of the diesel and methanol fuels [43]; (4) the power output per cylinder is assumed to be the same for all the engine cylinders.

The SAGE combustion model with the default values for its constants was employed for both the diesel and dual-fuel modes. A two-dimension adaptive zoning that conserves the NOx emissions during species

Table 1
Marine engine characteristics.

Parameter	Value
Type	Wärtsilä 9L46C
Brake power at MCR point (kW)	10,500
Speed at MCR point (r/min)	500
Cylinders Number (–)	9
Compression ratio	14.0:1
Bore/Stroke (mm)	460/580
Diesel start of injection (°CA BTDC)	6
Diesel injection pressure (bar)	1,200
Methanol energy fraction (%)	90
Nozzle angle (deg)	67.5
Spray cone angle (deg)	17.5
Nozzle diameter (mm)	0.78
Nozzle holes number (–)	6
Simulated cycle period	IVC – EVO 135°CA BTDC–135°CA ATDC

Table 2
Optimisation variables.

Variable	
Temperature at IVC*	Group A
Pressure at IVC	
Compression Ratio	
Injection Method	
Injection Strategy	
Exhaust Gas Recirculation	Group B
Start of Injection	
Injection Duration	
Injection Pressure	
Spray characteristics (cone angle, size etc.)	

*IVC: inlet valve closing.

Table 3
Computational mesh characteristics.

Parameter	Grid 1	Grid 2	Grid 3	Grid 4
Base element size (mm)	8	8	8	8
Final element size (mm)	8	2	1	0.5
Solution duration (h)	4	11	20	70
RMSE on p_{cyl}* (MPa)	0.288	0.244	0.215	0.214
Error on p_{max} (%)*	6.2	4.4	1.3	3.4
Adaptive mesh refinement	On: between 12°CA BTDC and 135°CA ATDC			
Number of Cores Used	40: Intel Cores IPM			

*For the diesel operation mode; RMSE: root mean square error; p_{cyl}: in-cylinder pressure for the closed cycle; $p_{max:}$ maximum in-cylinder pressure.

remapping was used. A preconditioned, constant volume iterative solver was employed, with the relative tolerance equal to 0.0001, and the iteration error for each species equal to 10^{-14} [44]. The KH-RT spray break up model (considering the default values for its constants) was employed for the diesel and methanol direct injection. The RT model breakup time, model size and length constants were set to 1.0, 0.1, and 50, respectively. The KH model breakup time constant and model size constant was considered 7 and 0.61 respectively, shed factor is 1. These values were selected according to the previous studies of the authors based on spray validation using both diesel [45] and methanol [46] data.

2.2. Investigated engine

This study investigates a nine-cylinder marine medium-speed engine, with a maximum power output of 10.5 MW at 500 rev/m. The engine is used for propulsion (driving the propeller) in several ship types. The engine particulars are presented in Table 1, whereas the experimental procedure is discussed in authors previous studies [37]. The CFD model for the diesel mode considers the properties of marine gas oil (MGO). The diesel is directly injected in-cylinder close to TDC at 1200 bar according to the manufacturer guidelines.

2.3. Grid sensitivity study & experimental validation

A grid sensitivity study is conducted to determine the trade-off between error and computational time for both the diesel and dual fuel modes. The considered grids include a base element size of 8 mm, which is refined using adaptive mesh refinement (AMR) reaching 2 mm, 1 mm and 0.5 mm, for Grids 2, 3 and 4, respectively. Grid 1 is the base grid without AMR with 8 mm cell size. The characteristics of the considered computational meshes are listed in Table 3. The in-cylinder pressure, mean temperature, and heat release rate (for each grid) along with the available measured results (for the diesel mode) are presented in Fig. 3a and b for the diesel mode and the dual fuel mode with 90 % MEF at 30 % load. The relative error is calculated on the maximum in-cylinder pressure whereas the root mean square error (RMSE) is evaluated for all the pressure diagram against the experimental values. The results demonstrate that convergence is achieved, as Grids 3 and 4 exhibit only slight differences in the maximum in-cylinder pressure and heat release rate. Grid 4 exhibits reduced maximum in-cylinder temperature compared to Grid 3. For the dual fuel operation, convergence is achieved for Grid 3. Based on the presented results, it is deduced that Grid 3 (with elements size of 1 mm) is considered the best compromise between computational time and accuracy.

Fig. 4a presents the measured and simulated in-cylinder pressure and HRR for the considered marine engine operating at 30 % load. The error in the maximum in-cylinder pressure between the simulation and measurements is around 1 %, whereas the simulation results exhibit satisfactory agreement with the respective measurements. The error in the peak heat release rate is 4 %, whereas the simulated peak HRR is 1 % higher than the measured one. The differences between measured and simulated results are attributed to the cylinders degradation, as well as differences in the initial and boundary conditions [47]. However, it can be deduced that the CFD model for the diesel mode provides results with adequate accuracy.

As measurements for the considered marine engine operating with methanol operation were not available, measured data reported in the literature for a light-duty high-speed diesel engine operating in the dual fuel mode with 30 % MEF was employed to validate the CFD model for the methanol operation. Methanol is injected in the port, whereas the engine load is 75 %. Details of the experimental procedure and engine test bench is provided in Zang et al [48]. The in-cylinder pressure and heat release rate variations are presented in Fig. 4b for the dual-fuel operation. The error on maximum in-cylinder pressure (p_{max}) between experimental and simulated data is 0.5 % with a slight retard in the crank angle (CA) at p_{max} from 7.5 °CA ATDC to 11 °CA ATDC. The combustion efficiency for the dual fuel operation of the light-duty engine is 98 % in the experimental measurements whereas the simulated operation yielded 96.9 %. According to literature [49–52] the CFD models developed, and experimental data acquired follow similar trends with the ones provided in this study. The CFD models tend to overestimate the premixed part of the heat release rate by 2–10 % compared to the experimental data, whereas peak pressure is shifted between 2 and 5 °CA. Such literature data come in agreement with the ones retrieved from the current analysis. Based on these findings, the developed CFD models (for both the diesel and dual fuel models) are considered validated for the scope of this study.

In addition, the developed model is validated against experimental measurements obtained from the shop trials for the diesel mode and the dual-fuel mode with natural gas, which are presented in Tables A2 and A3 (Appendix A). Further details of the developed models are provided in authors previous studies [53,54].

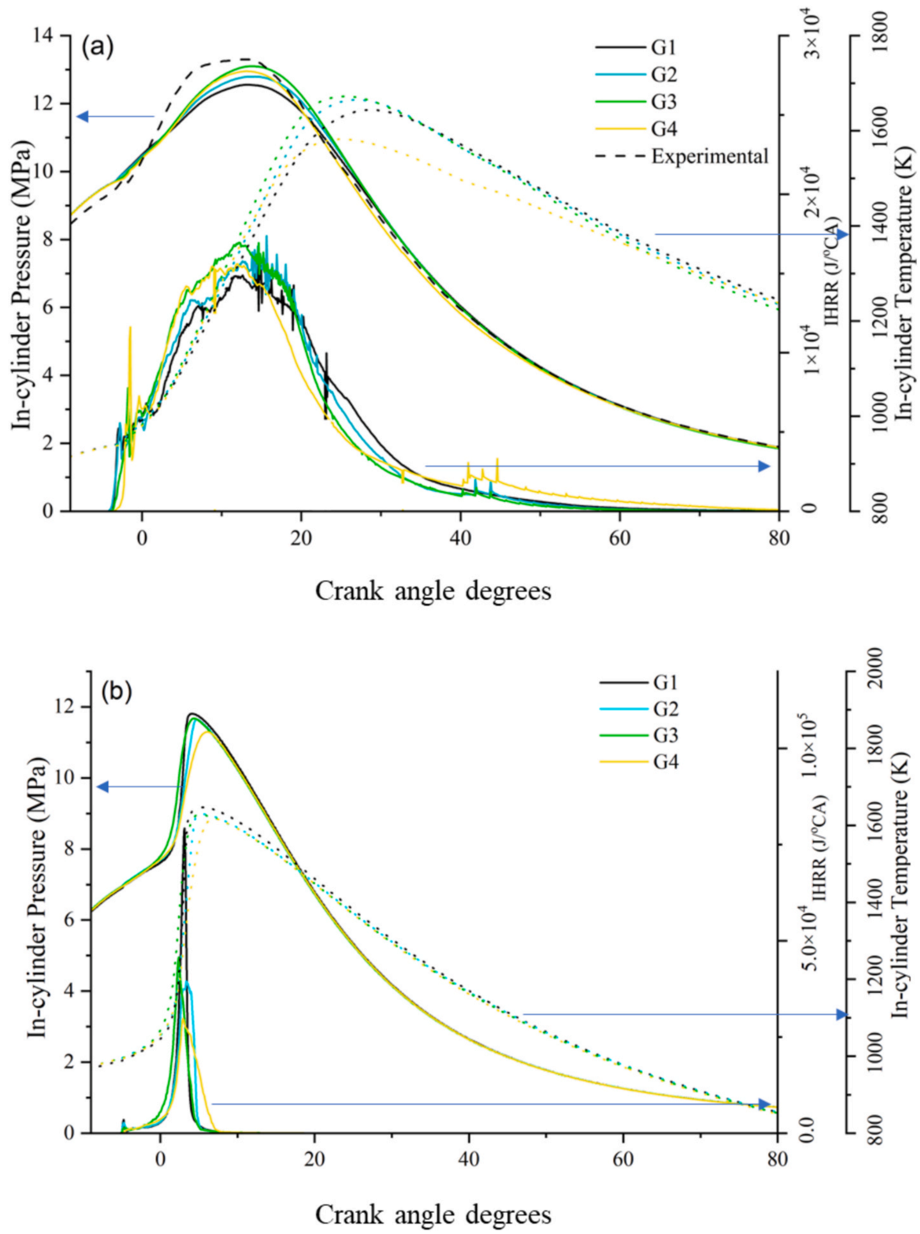

Fig. 3. In-cylinder pressure, heat release rate and mean in-cylinder temperature variation for the selected grids; (a) diesel mode, and (b) dual-fuel mode.

2.4. Injection strategies

This study considers the two-stage, thee-stage, and stratified injection strategies to mitigate the single injection strategy limitations at low loads. The single injection strategy results in methanol injection during the compression stroke (SOI: 50°CA BTDC), to achieve homogeneous methanol–air mixture. The pilot diesel is injected close to TDC to initiate combustion (Fig. 5a). Single methanol injection is effective at medium and high loads, as reported in [37]. However, in low-load conditions with reduced intake temperatures, the 10 % diesel energy fraction is not sufficient to ignite the air-methanol mixture, as considerable heat is absorbed due to the methanol evaporation, leading to reduction of the in-cylinder temperature and reactivity.

The two-stage methanol injection strategy, which is schematically illustrated in Fig. 5b, entails: (a) injecting half of the total methanol mass during the compression stroke, (b) the same pilot diesel injection timing with that of the single-stage strategy is employed to initiate combustion around 3 °CA BTDC, and (c) the remaining two-thirds of the methanol fuel is injected 0–8 °CA ATDC. Injecting half methanol mass early during the stroke, ensures better mixing with air benefitting the combustion process [54] whereas the rest of methanol is injected close to TDC just after diesel with the aim to achieve mixing control combustion to moderate peak heat release rate. The suggested range was the outcome of initial simulations that explored a feasible operating envelope. The limitations of this strategy are elaborated in the results section.

The three-stage methanol injection strategy, which reduces NOx emissions [55], is shown in Fig. 5c. The methanol injection after TDC is split in two different injections between 0 and 4 °CA ATDC and 5–9 °CA ATDC. The combustion starts close to TDC as the lower methanol mass (at each injection stage) reduces the quenching effect. The diffusive flame front results in the combustion of the methanol injected in the third stage between 5 and 9 °CA ATDC. The adopted injection ratio follows the principle of providing a strong initial premixed foundation while staging the remaining methanol to control the combustion phasing. The first 50 % injection during the compression stroke establishes a reactive charge that the diesel pilot can ignite reliably, especially at low load operation where reactivity is reduced in-cylinder. The subsequent two 25 % injections, delivered shortly after TDC, extend the

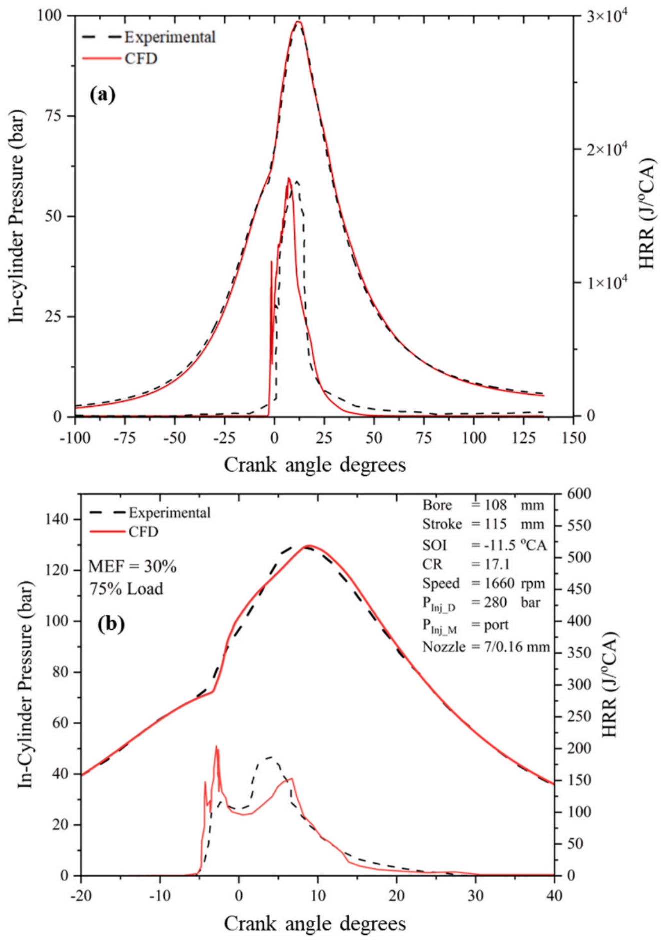

Fig. 4. Experimental and CFD model results for the in-cylinder pressure and heat release rate for: (a) the considered marine engine operating in diesel mode, and; (b) a light duty engine operating with 30% MEF.

combustion duration and moderate the heat release rate [56].

The stratified injection strategy is achieved by a single injector as shown in Fig. 6. The stratified injection is modelled by configuring different injection rate-shape profiles for both fuels. The injected energy remains constant, whereas the diesel and methanol fuels are injected in three stages with energy shares of 50 %, 25 % and 25 % for diesel and 20 %, 40 % and 40 % for methanol. The relatively small initial methanol fraction (20 % of the total methanol amount) prevents excessive cooling of the in-cylinder charge and avoids quenching of the diesel pilot flame, while also reducing the risk of spray wall impingement near TDC. The subsequent larger fractions (40 % and 40 %) are injected after the diesel fuel injections and stable flame fronts formations, ensuring that methanol combustion proceeds in a controlled diffusive manner [57]. Both fuels injection pressure was set to1200 bar for the single, two- and three-stage injection strategies, and 600 bar for the stratified injection strategy. All the injection parameters considered in the study are listed in Table A4 (Appendix).

2.5. Cases description

The developed dual-fuel model considers the methanol direct injection to substitute 90 % of the diesel energy (i.e., 90 % MEF) and 10 % pilot diesel energy fraction (to initiate combustion). Both fuels are directly injected in-cylinder, as diffusive combustion is preferred to reactivity-controlled compression ignition (RCCI) for high MEF values [58,59]. The injection parameters are listed in Table A4.

The start of combustion is associated with the in-cylinder reactivity, which depends on temperature and pressure. The examined parameters are the temperature at inlet valve closing (T_{IVC}) and the compression ratio (CR), with their considered ranges being 14–17 for CR (14 is the diesel engine CR), and 360–400 K for T_{IVC}.

The considered cases are listed in Table 4. The higher T_{IVC} can be is achieved by controlling the charge air cooler cooling water flow. The initial conditions with T_{IVC} of 360 K and CR of 14 refer to the marine diesel engine operation (baseline).

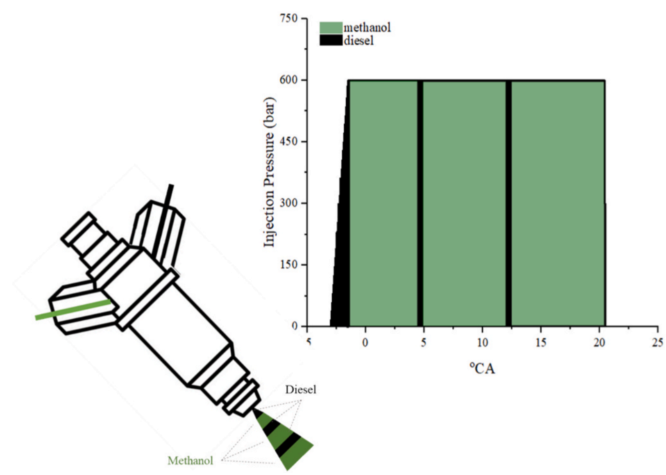

Fig. 6. Methanol–diesel stratified injection strategy along with the rate shape profile.

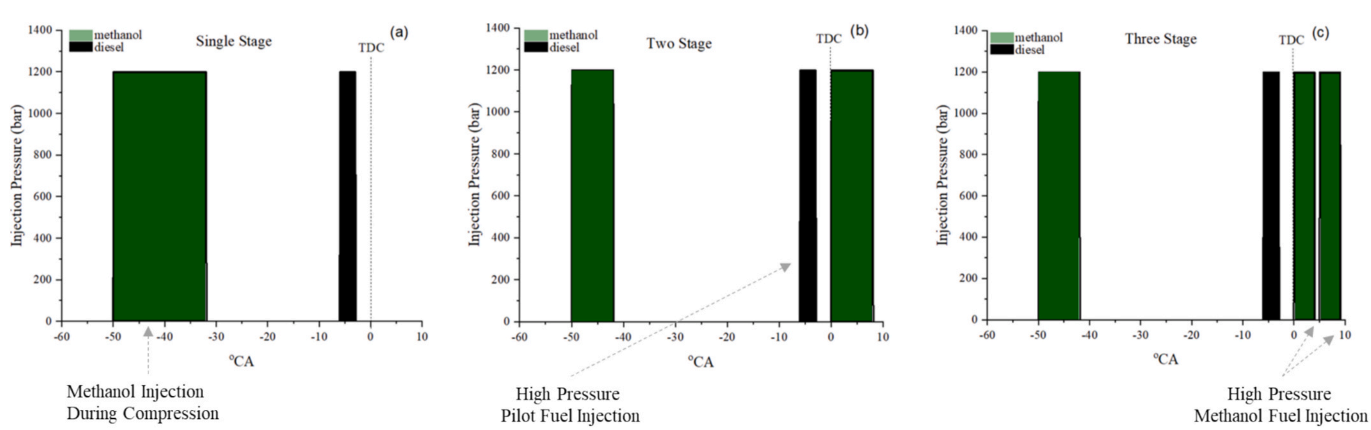

Fig. 5. Methanol, single (a), two-stage (b) and three-stage (c) injection strategies.

Table 4
Conditions and settings for the investigated cases for 30% engine load.

Case	T_{IVC} (K)	CR	Injection Strategies* 1S	2S	3S	ST	Rationale
BL	360	14	x				Baseline diesel operation
1	360	14	x	x	x	x	Higher T_{IVC} improves in-cylinder
2	380	14	x	x	x	x	reactivity for constant CR.
3	400	14	x	x	x	x	
4	360	15	x	x	x	x	Higher T_{IVC} and CR further
5	380	15	x	x	x	x	improves reactivity, as methanol
6	400	15	x	x	x	x	quenching characteristics inhibits
7	360	16	x	x	x		combustion at low loads.
8	380	16	x	x			
9	400	16	x	x	x	x	
10	360	17	x	x	x		
11	380	17	x	x	x		
12	400	17	x	x	x	x	

1S: one-stage (single) injection, 2S: two-stage injection, 3S: three-stage injection, ST: stratified injection.

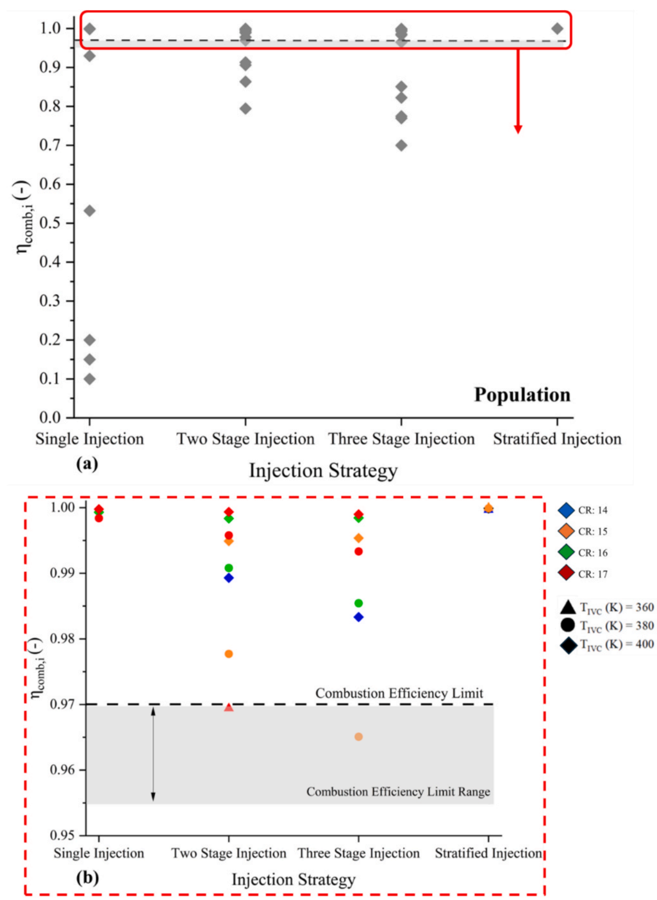

Fig. 7. Derived combustion efficiency: (a) for all the investigated cases; (b) for the cases that satisfy the combustion efficiency constraint.

3. Results

This section presents and discusses the results from the considered cases to determine the effects of the injection strategies and initial conditions on the engine performance, and emissions parameters. Three-dimensional distributions of temperature, NOx, and fuel mass fractions are also presented and commented.

3.1. Parametric optimisation

The parametric optimisation included 42 cases (and respective simulation runs). The constraint set for the combustion efficiency was 97 %, however, due to the uncertainties in CFD simulation results, cases with combustion efficiency above 95.5 % were analysed. Fig. 7(a) presents the derived combustion efficiency for the considered injection strategies. Fig. 7(b) presents the combustion efficiency for the 22 cases satisfying the combustion efficiency constraint.

For the single injection strategy, three cases satisfied the set constraint, which exhibit high values for the CR and T_{IVC}. For the two-stage injection eight cases were identified with CR and T_{IVC} in the ranges 14–17 and 360–400 K, respectively. For three-stage injection, seven cases were identified with CR and T_{IVC} in the ranges 14–17 and 380–400 K. For stratified injection, all the examined cases satisfied the set combustion efficiency constraint.

The single injection strategy requires high values of CR and T_{IVC} and to achieve increased in-cylinder reactivity facilitating improved reaction kinetics in-cylinder, leading to close to complete combustion conditions ($\eta_c > 99$ %). At lower CRs and $T_{IVC,}$ while combustion starts, the energy provided from pilot diesel combustion fails to result in unacceptable methanol combustion efficiency due to the high vaporisation heat and mass of the injected methanol, hence quenching the diesel flame front.

For the two-stage injection strategy, as half of methanol mass is injected prior to diesel, the flame front is sustained further. Therefore, the minimum combustion efficiency constraint was satisfied for cases with lower values of CR and $T_{IVC.}$ However, the methanol second injection that takes place after TDC, results in reduced combustion efficiency for low CR and $T_{IVC.}$ Similar behaviour is exhibited with the three-stage injection. As only one third from the total methanol amount is injected during the compression stroke, the pilot diesel combustion is adequate to initiate the methanol combustion. However, high T_{IVC} is required so that the 2nd and 3rd methanol injected batches combust effectively. Stratified injection leads to close to complete combustion at reduced CR and T_{IVC}, as the established in-cylinder conditions facilitate the effective combustion of the consecutively injected batches of diesel and methanol.

Fig. 8 illustrates the distributions of the thermal efficiency, NOx emissions and unburned methanol (UM) for the cases satisfying the combustion efficiency constraint. For the indicated thermal efficiency, most cases concentrate close to 49 % ($1-\eta_{th,i} = 0.51$) indicating that there are a few cases with very low or high thermal efficiency values. The NOx distribution indicates higher variability among the NOx emissions implying greater sensitivity towards injection strategy and initial conditions. While the median is around 8 g/kWh, the derived NOx range is between 4 to 16 g/kWh. The narrow range of UM distribution indicates that all qualified cases exhibit low unburned methanol emissions. The upper limit of the UM emissions that correspond to the combustion efficiency constraint of 99.7 % is 4.5 g/kWh.

Fig. 9(a) presents the indicated thermal efficiency and NOx emissions objectives. Fig. 9(b) illustrates the objectives of the indicated thermal efficiency and unburned methanol emissions. Fig. 9(c) demonstrates the objectives of NOx and indicated thermal efficiency are presented along with contours for the UM emissions.

All the presented cases exhibit higher efficiency and lower NOx emissions from the baseline diesel operation. The results showcase the four injection strategies form three clusters. The single injection strategy cluster exhibits NOx emissions between 7.2 and 9.3 g/kWh whereas the indicated thermal efficiency is between 52.5 and 53.5 % ($1-\eta_{th,i}$ = 0.475–0.465). The stratified injection (top-left) exhibits reduced NOx emissions and thermal efficiency ranging in 4.6–7.5 g/kWh and 47–48.3 %, respectively. The two and three stage injection strategies form a common cluster; the NOx emissions and indicated thermal efficiency span between 9.6 to 14.7 g/kWh and 47.5 to 50 %, respectively.

For the single injection strategy, the high CR values (16 and 17) result in greater indicated thermal efficiency due to increased work

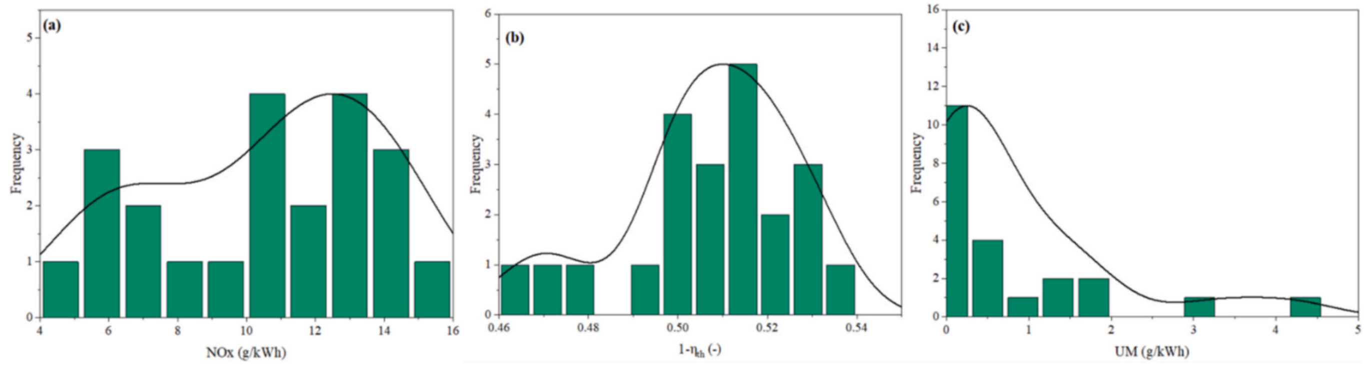

Fig. 8. Distributions of the (a) NOx emissions; (b) indicated thermal efficiency, and (c) unburned methanol emissions.

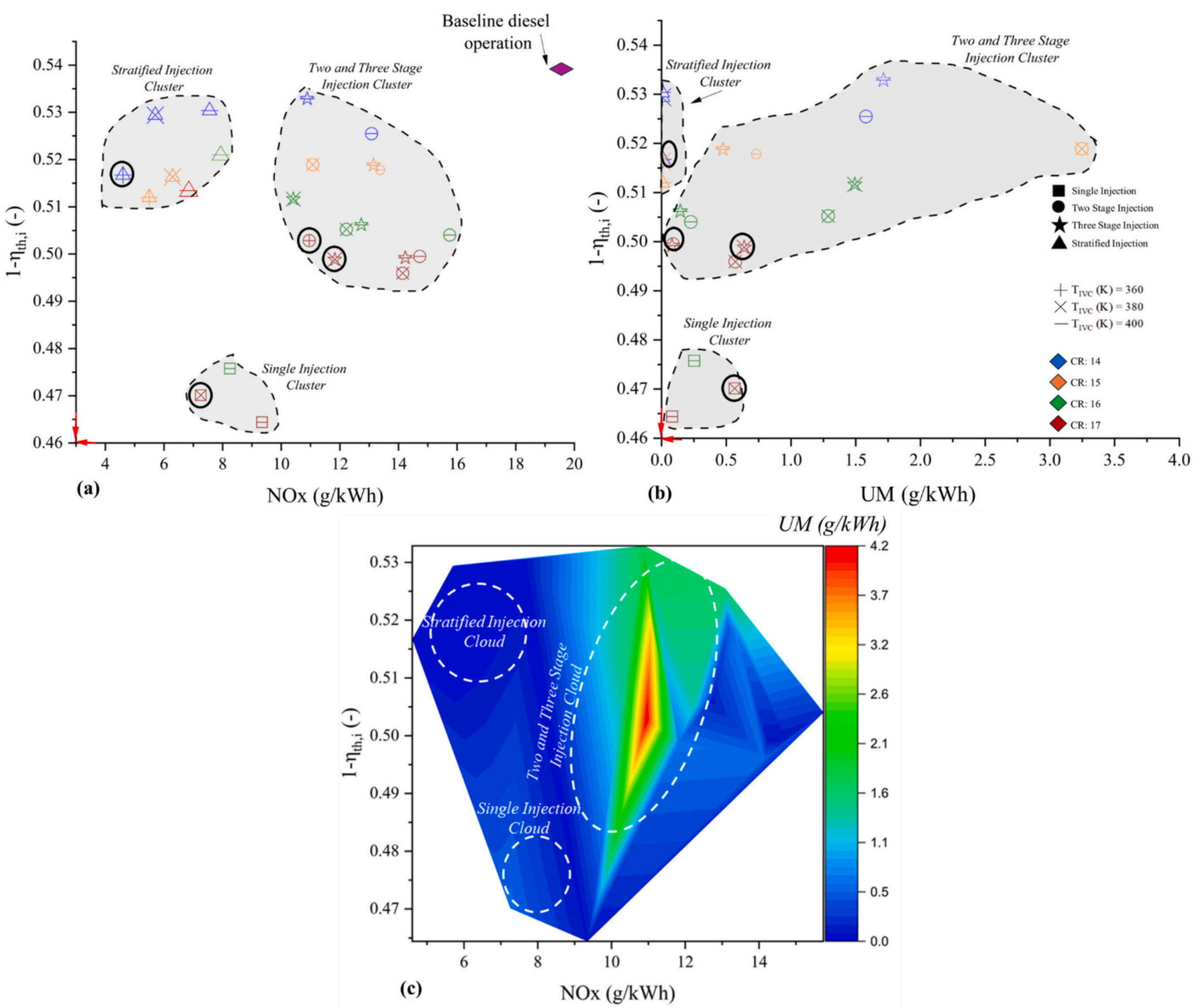

Fig. 9. Parametric runs results for the three employed objectives: (a) Indicated thermal efficiency versus NOx emissions; (b) Indicated thermal efficiency versus unburned methanol; (c) indicated thermal efficiency versus NOx emission with superimposed contours for unburned methanol emissions.

produced during the expansion phase of the closed cycle. Furthermore, increased T_{IVC} (380 and 400 K) results in shorter combustion duration yielding thermal efficiency improvement. The single injection strategies cases exhibit smaller thermal efficiency variation, hence, Case 12 (CR = 17 and T_{IVC} = 400 K) that has the lowest NOx emissions was selected as optimal.

The stratified injection cases exhibit low NOx emissions at low CR and T_{IVC} due to the lower in-cylinder temperature conditions. Both fuels

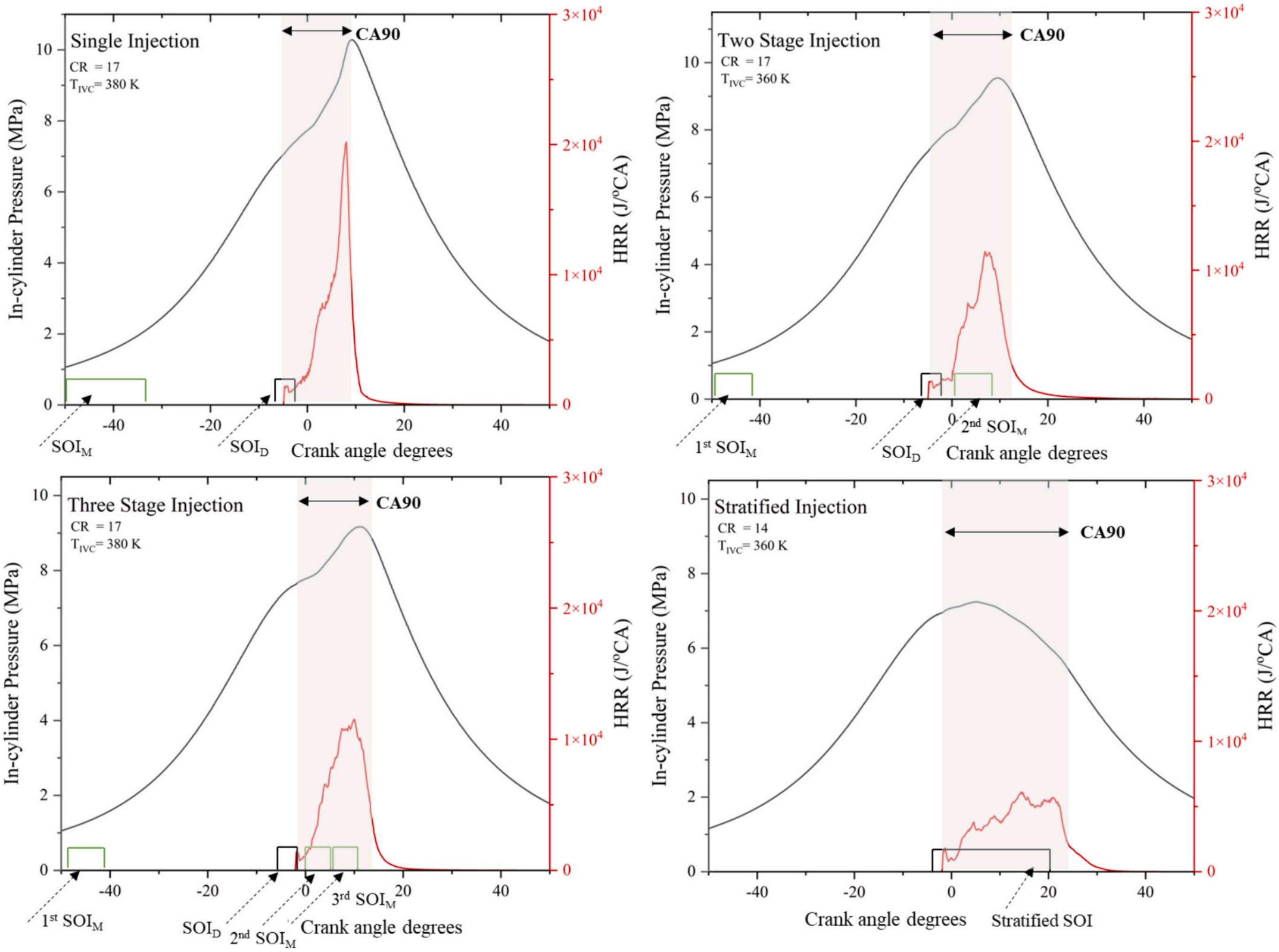

Fig. 10. In-cylinder pressure and heat release rate for the selected optimal cases of the different injection strategies.

combustion occurs diffusively in a slower rate compares to the other injection strategy (lower HRR values), resulting in lower maximum in-cylinder pressure and thermal efficiency. Since thermal efficiency does not significantly increase with the increase of CR, Case 1 (CR = 14 and T_{IVC} = 360 K) exhibiting the lowest NOx emissions was selected as optimal.

For the two- and three-stage injection strategies, the indicated thermal efficiency increases with CR reaching close to 50 %, whereas higher T_{IVC} results in higher NOx emissions. Hence, for the two-stage injection, Case 10 (CR = 17 and T_{IVC} = 360 K) exhibiting the lowest NOx emissions was selected as optimal. For the three-stage injection, Case 11 (CR = 17 and T_{IVC} = 380 K) was selected as optimal, as it exhibited the highest thermal efficiency and the lowest NOx emissions.

The selected optimal cases for each injection strategy exhibit UM emissions well below the 4 g/kWh threshold; 0.59 g/kWh for the single injection strategy, 0.65 g/kWh for three-stage injection strategy, almost 0 g/kWh for two-stage and stratified injection strategies indicating close to complete combustion conditions (η_c > 99.5 %).

3.2. Engine performance and emissions parameters

Fig. 10 shows the crank angle variations of the in-cylinder pressure and heat release rate for the selected optimal cases for each injection strategy, whilst providing information for the start of injection for methanol and diesel fuels and the combustion duration as represented by CA90 (which denotes the CA where 90 % of the combustion is completed). Fig. 11 shows the crank angle variation of the in-cylinder maximum temperature, NOx mass and methanol mass for the selected optimal case for each injection strategy.

For the single injection strategy, the maximum in-cylinder pressure and peak heat release rate are 9.9 MPa and 21.1 kJ/°CA, respectively. The first peak in HRR is attributed to the pilot diesel fuel combustion. As methanol has significantly higher laminar flame speed than diesel fuel, high T_{IVC} and CR, the combustion occurs rapidly, resulting in CA90 close to 10 °CA ATDC. The rapid combustion of methanol results in fast increase of the maximum in-cylinder temperature (due to high CR and T_{IVC}). However, the in-cylinder mixture residence above 1800 K (NOx cut-off temperature) is shorter (compared to the two- and three-stage injection), resulting in lower NOx emissions.

For the two-stage injection strategy, the pilot diesel started the combustion of the first injected methanol part (injected at 50 °CA BTDC) resulting in the first peak at the HRR at 2 °CA ATDC, which is followed by a period of gradual HRR increase, prior to the second methanol injection. At 0°CA (TDC), the second part of methanol injection starts, and its diffusive combustion occurs, leading to the maximum HRR value (11.4 kJ/°CA at 8 °CA ATDC), yielding maximum in-cylinder pressure of 9.52 MPa. The combustion duration is extended compared to the single injection strategy, with CA90 being exhibited at 12.7 °CA ATDC, resulting in prolonged high temperature period, and increased NOx emissions to 11 g/kWh compared to 5.3 g/kWh for the single stage injection. According to Fig. 11b, despite the longer duration of the in-cylinder mixture at elevated temperature, for stratified injection, the

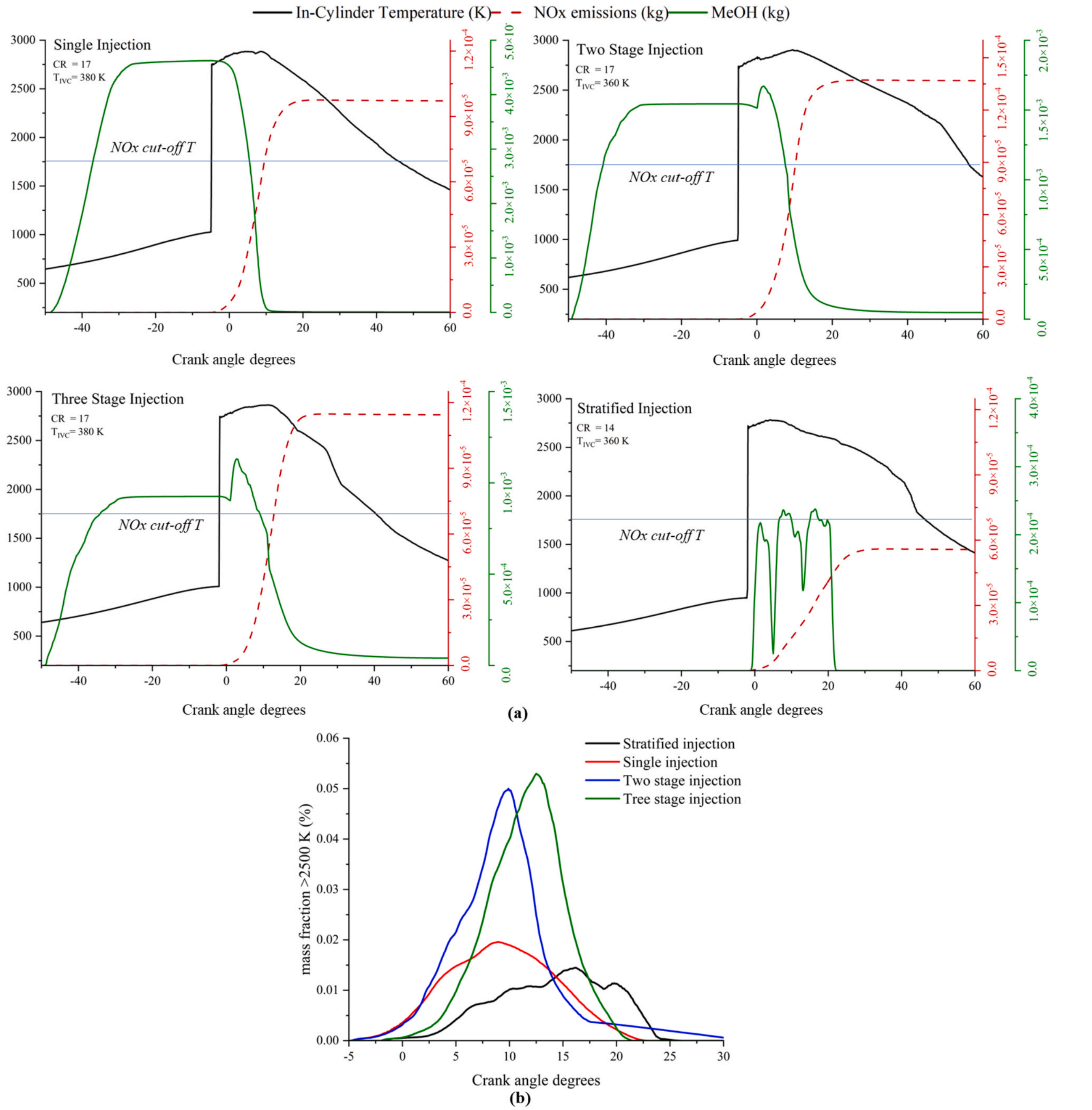

Fig. 11. (a) Crank angle variations of the in-cylinder maximum temperature NOx mass, and methanol mass for the selected optimal cases for each injection strategy and (b) in-cylinder mass fraction at temperature higher than 2500 K.

mass fraction is lower than in other injection strategies yielding lower NOx emissions. The requirement for elevated CR negatively affects NOx creation.

For the three-stage injection strategy, maximum in-cylinder pressure is 9.16 MPa and peak HRR 11.3 kJ/°CA. This is due to the prolonged injection of methanol fuel. This case demonstrates longer ignition delay compared to the single and two-stage injection, while CA90 occurs at 13.8 °CA ATDC. For all the split injection strategies, the heat release rate indicates limited premixed combustion periods, due to the direct injection of both diesel and methanol. The extended combustion duration (compared to the other strategies). The longer combustion duration, results in considerable period with high in-cylinder temperature values, leading to high NOx emissions (11.8 g/kWh) compared to two and single injection strategies (11 and 5.3 g/kWh, respectively).

For the stratified injection strategy, a 2 °CA ignition delay is observed. The maximum pressure is considerably lower than the other injection strategies, hence the expected thermal efficiency is lower. The first HRR peak appears at 2°CA BTDC, and is attributed to the diesel combustion, whereas four more peaks are observed at 5°CA, 10°CA, 15°CA and 20°CA ATDC. These are attributed to the 1st batch of diesel, 2nd batch of methanol, 3rd batch of diesel and final batch of methanol. After the diesel injection end, the recuring methanol injection effectively limits the significant in-cylinder temperature increase. The peak HRR and in-cylinder pressure reached 6.1kJ/°CA and 7.24 MPa respectively, whereas CA90 occurs at 23 °CA ATDC. The prolonged combustion and the shift of the peak heat release rate from the typical CA values (10 °CA

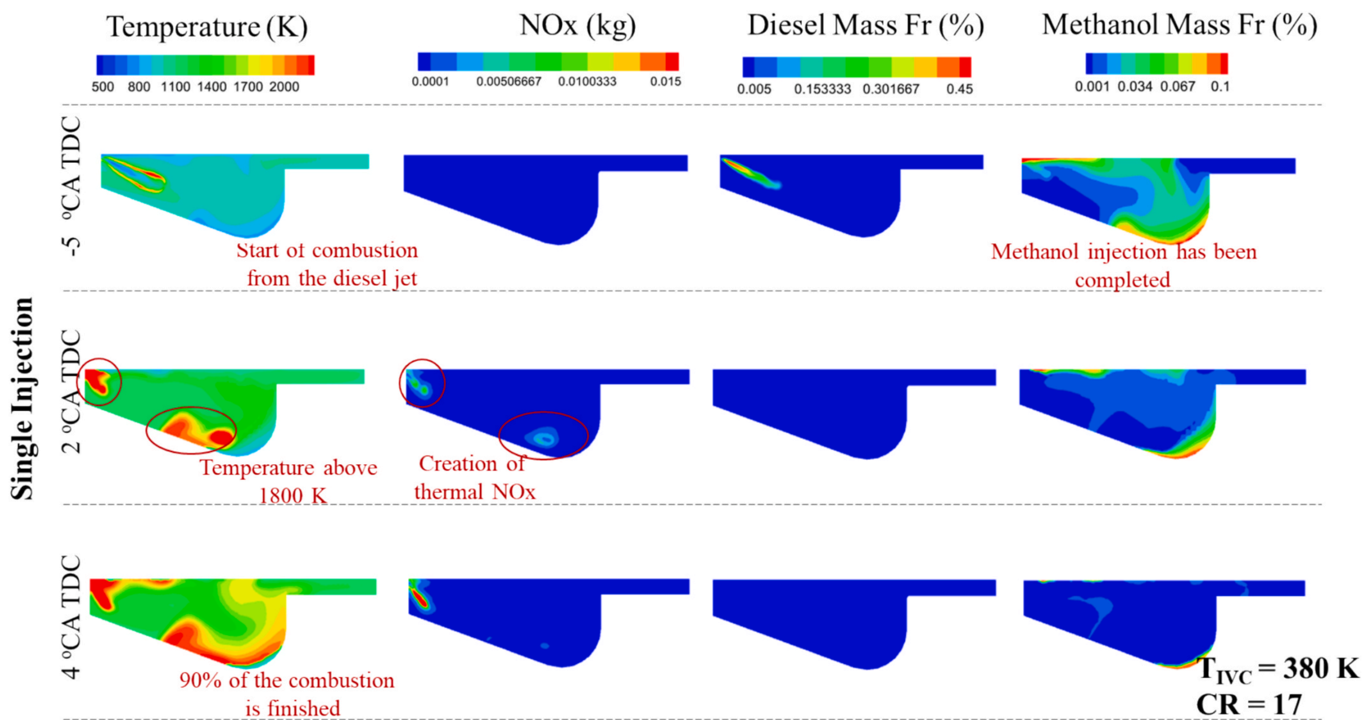

Fig. 12. Contours of in-cylinder temperature, NOx, diesel and methanol mass fractions for the optimal case of the single injection strategy.

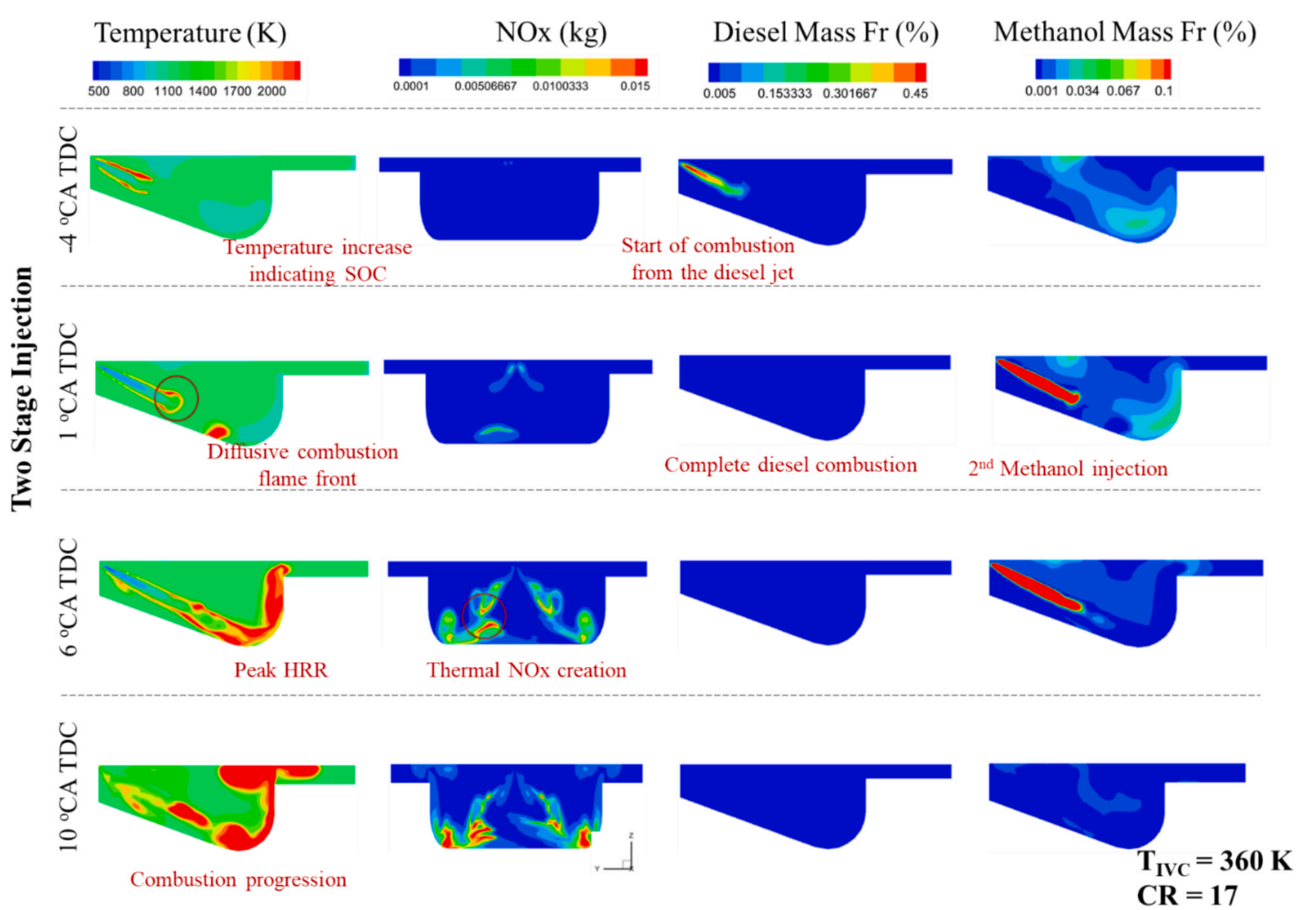

Fig. 13. Contours of in-cylinder temperature, NOx, diesel and methanol mass fractions for the optimal case of the two-stage injection strategy.

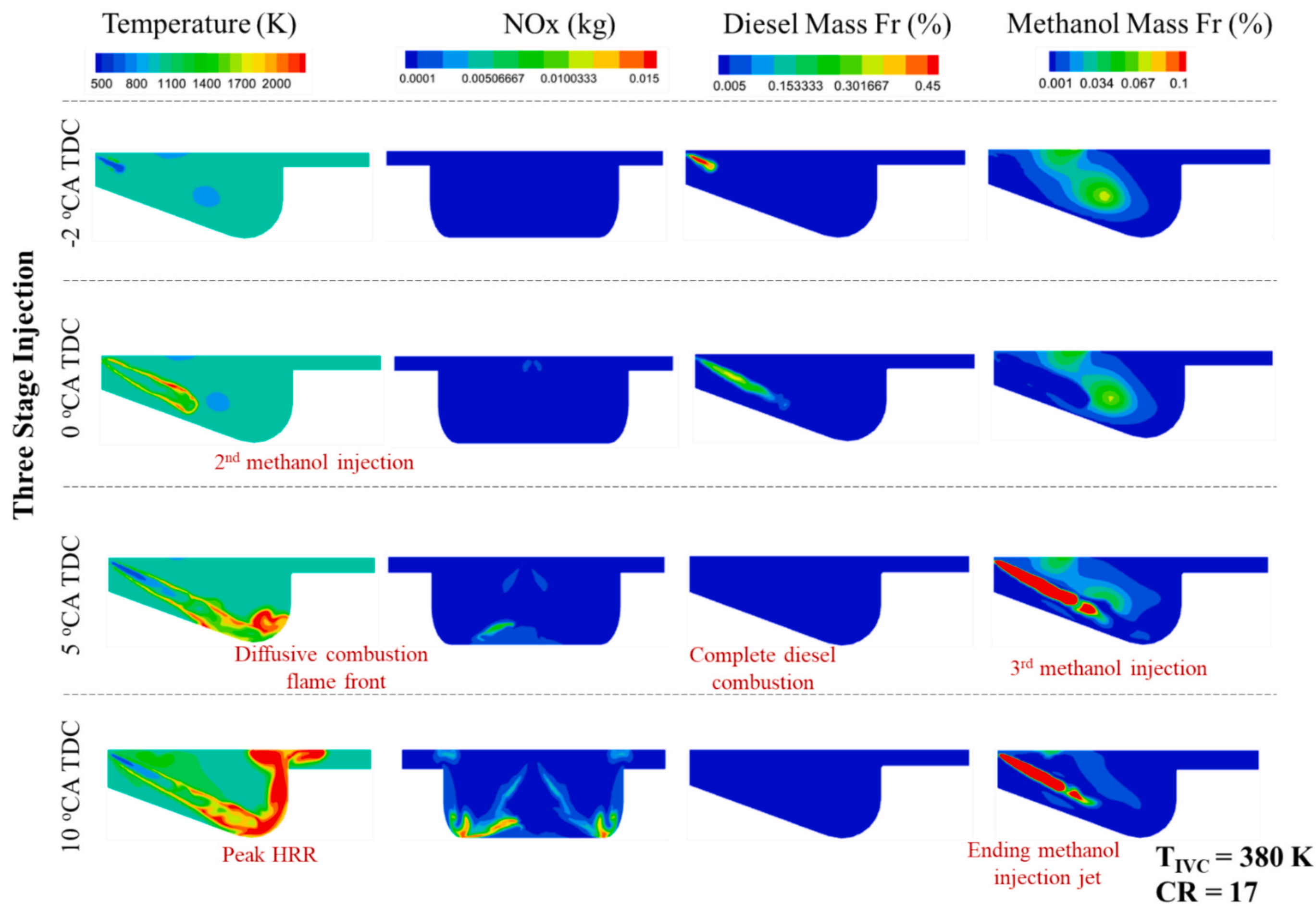

Fig. 14. Contours of in-cylinder temperature, NOx, diesel and methanol mass fractions for the optimal case of the three-stage injection strategy.

according to Ref. [60]) lead to lower in-cylinder maximum pressure and thermal efficiency. The stratified injection facilitated the relatively slow (but effective) methanol combustion (following each diesel batch injection and combustion) leading to reduced maximum in-cylinder temperature (to 2700 K), and hence significantly decreasing the working medium residency time at high temperatures, which in turn results in reduced NOx emissions.

Fig. 11(b) demonstrates that the in-cylinder mixture (reaction products) mass fraction that is exposed to temperatures above 2500 K is lower for the stratified injection compared to the other injection strategies. This justifies the reduced NOx emissions for the stratified injection case. Furthermore, the injected diesel forms ignition kernels of high reactivity, whereas the injected methanol results in the reaction zones cooling and flame quenching. On the contrary, for the other injection strategies, the larger homogeneous regions exposed to at very high temperatures leads to higher NOx emissions.

3.3. In-cylinder parameters spatial analysis

This section presents the derived three-dimensional variation for the in-cylinder temperature, NOx emissions, diesel and methanol mass fractions for the selected optimal cases of each injection strategy. The comparison between injection strategies is facilitated benchmarking same combustion phases such as start of combustion, methanol injections, peak HRR and CA90. Fig. 12 shows the parameters contours for the single stage injection strategy. The combustion starts at 5 °CA BTDC, where methanol is not homogenously mixed with air as in-cylinder local rich regions are formed (in the vicinity of the piston bowl and cylinder head walls). This is a potential area for prompt NOx formation, however since temperature is above 2000 K in this region, NOx concentration is mostly affected by thermal NOx creation. At 2 °CA ATDC, the temperature exceeds the NOx cutoff temperature (1800 K) in areas close to rich methanol concentration. Therefore, the thermal NOx onset areas (where the air nitrogen oxidates to N_2O and NO) appear in Fig. 12. At 4 °CA ATDC, 90 % of the combustion is completed with a small amount of unburnt methanol remaining in the vicinity of the piston bowl.

Fig. 13 shows the parameters contours for the two-stage injection strategy at different crank angles. At 4 °CA BTDC, the diesel combustion starts, as indicated by the temperature increase in the jet interface. As only half of the total methanol amount is injected, the methanol mass fraction is lower compared to the single injection strategy. During the second methanol injection starting at 1 °CA ATDC, a clear diffusive flame front is apparent from the temperature contours. At 6 °CA ATDC, the peak heat release rate occurs as methanol injection ends, and NOx rich regions begin to form in areas close to the piston bowl, where combustion takes place. At 10 °CA ATDC, the combustion propagates and CA90 is reached whereas the NOx is still generated, till the in-cylinder temperature reduces below 1800 K (this occurs after 20 °CA ATDC).

The parameters contours for the three-stage injection parameters are presented in Fig. 14. For 0 °CA TDC, only the first injection of methanol has taken place and locally rich in methanol zones are formed in-cylinder. The greatest difference compared to the two-stage injection strategy is that the third methanol injection quenches the combustion flame at 5 °CA ATDC reducing the heat release rate and hence the combustion efficiency. However, the quenching effect leads to a slight reduction of the NOx emissions as shown for the results at 10 °CA ATDC.

Fig. 15 illustrates the parameters distributions for the stratified

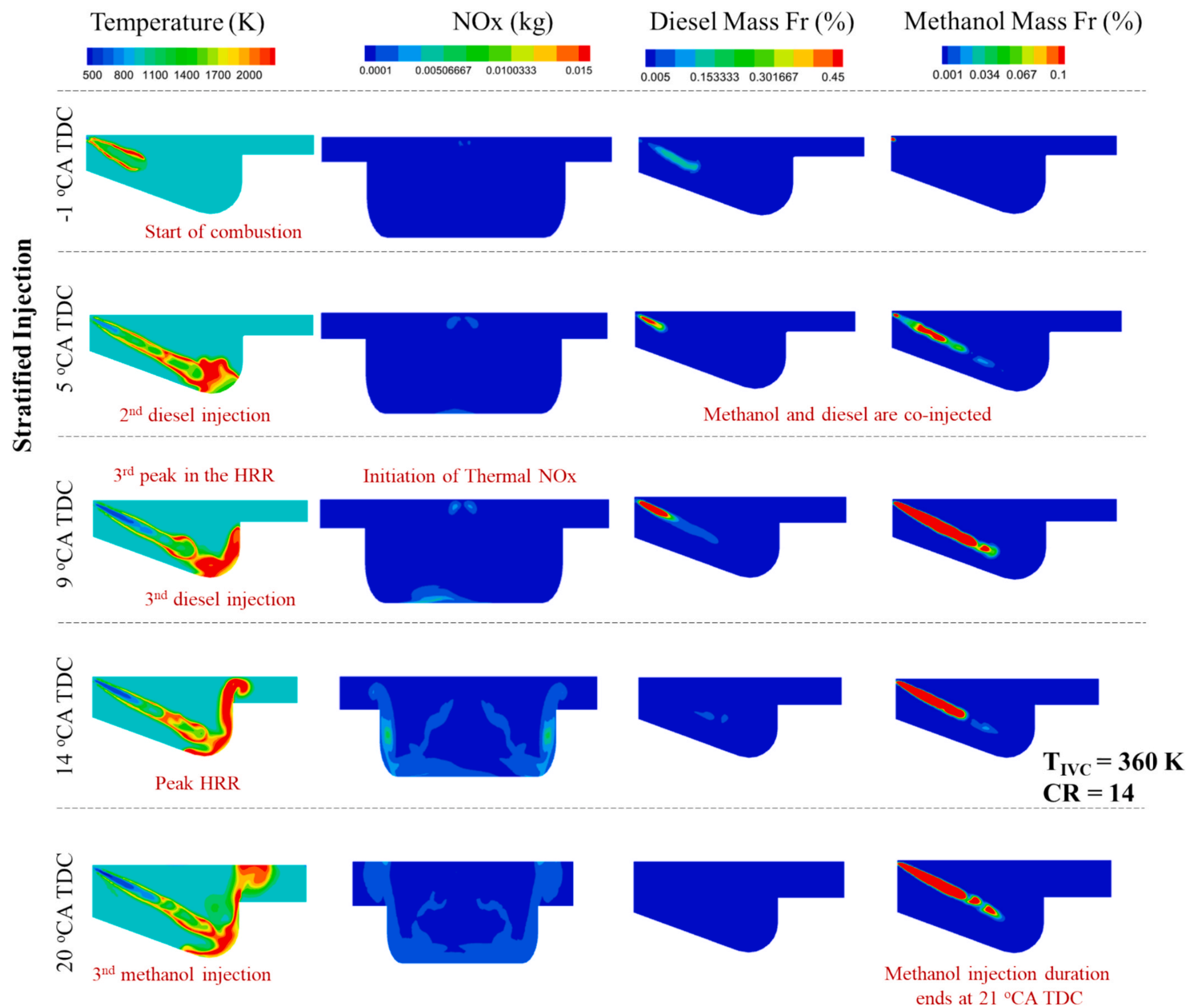

Fig. 15. Contours of in-cylinder temperature, NOx, diesel and methanol mass fractions for the optimal case of the stratified injection strategy.

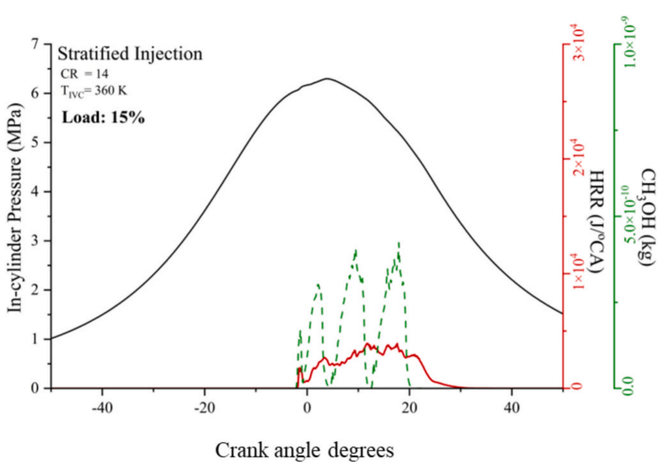

Fig. 16. In-cylinder pressure, heat release rate and methanol mass for the stratified injection for 15%.

Table A1
CFD models characteristics.

Mechanism	Diesel Mode	DF Methanol DI
Reaction Mechanism	Andrae and Head [42]	
Combustion	SAGE detailed chemistry	
NOx Mechanism	Extended Zeldovich [38]: Thermal NOx model; Mass scaling factor to convert NO to NOx: 1.533	
Turbulence Model	RANS RNG k-ε [61,62]	
Droplet breakup	KH-RT: The RT model breakup time, model size and length constants were set to 1.0, 0.1, and 50, respectively. The KH model breakup time constant and model size constant was considered 7 and 0.61 respectively, shed factor is 1, [45,46]	
	Mass diffusivity constants	
	C_7H_{16} $D_0 = 5.94 \times 10^{-6} n_0 = 1.6$	C_7H_{16} $D_0 = 5.94 \times 10^{-6} n_0 = 1.6$ CH_3OH $D_0 = 7.9 \times 10^{-6} n_0 = 1.87$
Droplets collision model	NTC [63]	
Wall heat transfer	Han & Reitz [64]	
Spray/Wall interaction model	O'Rourke [65]	

Table A2
Shop tests validation of maximum in-cylinder pressure, power output and NO emissions for the considered marine engine.

Load (%)	Maximum pressure			Indicated power output			NO emissions		
	Measured (bar)	CFD (bar)	Error (%)	Measured (kW)	CFD (kW)	Error (%)	Measured (ppm)	CFD (ppm)	Error (%)
50	135	135.4	0.3	4725	4900	4.6	9679	10,500	8.9
70	156	160	2.6	7088	6850	3.4	9296	10,100	8.0
100	205	204	0.5	9450	9440	1.0	9179	9390	3.3

Table A3
Shop test trials validation of the marine engine operating with natural gas.

Load	Indicated Power Output (kW)			Maximum cylinder Pressure (bar)			NOx emissions (g/kWh)		
	Measured	Simulation	Error (%)	Measured	Simulation	Error (%)	Measured	Simulation	Error (%)
25 %	1950	1900	3.6	38	38	0	9.15	9.9	8.6
50 %	3900	3950	2.3	64	66	4.1	9.7	10.1	4
75 %	5850	5700	3.6	92	90	3.2	9.7	10.4	7.8
100 %	7800	7890	2.2	126	125	1.8	9.43	10	6.7

Table A4
Injection parameters considered in the study.

Injection Method	Mass of Diesel/ Methanol (mg)	Injection Duration of Diesel (^{o}CA)	Injection Duration of Methanol (^{o}CA)	Injection Pressure of Diesel/ Methanol (bar)
SI	41/778	3	19	1200
TWI	41/ 259, 519		8, 8	
THS	41/ 156, 311, 311		8, 5, 5	
Str	20.5, 10.3, 10.3/158, 310, 310	1.5, 0.45, 0.45	6, 7.5, 7.5	600

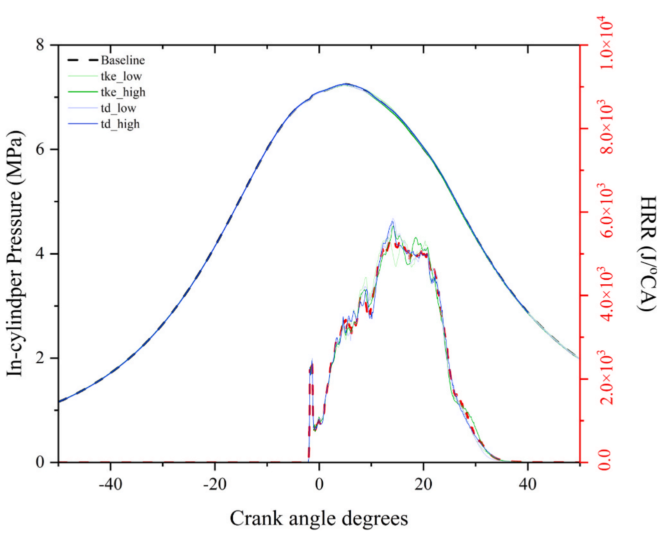

Fig. A1. In-cylinder pressure and heat release rate for the optimal stratified injection case under variable tke and td.

injection strategy. Overall, the NOx concentration is lower compared to other cases, due to the lower in-cylinder temperature. The latter is attributed to the quenching effect of methanol fuel. Every batch of injected diesel (with injection durations close to 1°CA) initiates a local diffusive flame front as it is observed at 1 °CA BTDC, 5 °CA ATDC and 9 °CA ATDC. Methanol that is injected directly after the diesel batch, quenches the flame front, as significant amount of energy is required to evaporate and as a result, reduces the maximum temperature. However, combustion efficiency is not penalised due to continuous reactivity

Table A5
Indicated thermal efficiency influencing parameters considered for the sensitivity analysis.

Sub-Model	Parameter	Examined extreme values
Geometry	Compression Ratio	12/19
Boundary Conditions	Piston Temperature (K)	300/600
	Cylinder Wall Temperature (K)	300/600
Initial Conditions	Temperature IVC (K)	200/400
	Pressure IVC (bar)	1/ 4
	Turbulent Kinetic Energy ($m^2/s^{2)}$	10/100
	Turbulent Dissipation (m^3/s^3)	10,000/30,000
Injection settings	Start of Injection Main Fuel (^{o}CA BTDC)	100/0
	Start of Injection Pilot Fuel (^{o}CA BTDC)	20/0
	Injection Duration Main Fuel (^{o}CA)	50/70
	Injection Pressure Main Fuel (bar)	300/1500
	Spray Temperature (K)	100/400
	Spray Cone Angle (^{o})	5/20
	Spray Tilt Angle (^{o})	40/70

enhancement from the diesel injections. Furthermore, alternating injections of diesel and methanol create local zones with different ignition delays. Diesel provides ignition kernels with high reactivity, while methanol quenches and cools the reaction zones. This interplay avoids large homogeneous regions at very high temperatures, which would otherwise strongly favour NOx production.

To investigate the preceding findings validity for other operating points in the low load region, the simulation of the stratified injection strategy optimal case (CR = 14 and T_{IVC} = 360 K) was performed in 15 % load. Fig. 16 presents the derived results. The heat release rate is characterised by four peaks associated with the combustion of the consecutively injected methanol batches. Almost complete methanol combustion was exhibited. The derived results align with the results for 30 % load, verifying the stratified injection strategy leads to acceptable engine operation with high methanol energy fraction.

3.4. Discussion and study implications

This study identified optimal conditions for methanol-fuelled marine dual-fuel engines operating with 90 % methanol energy fraction, including CR and T_{IVC} to improve efficiency and reduce NOx emissions, whilst eliminating the unburnt methanol. The stratified injection

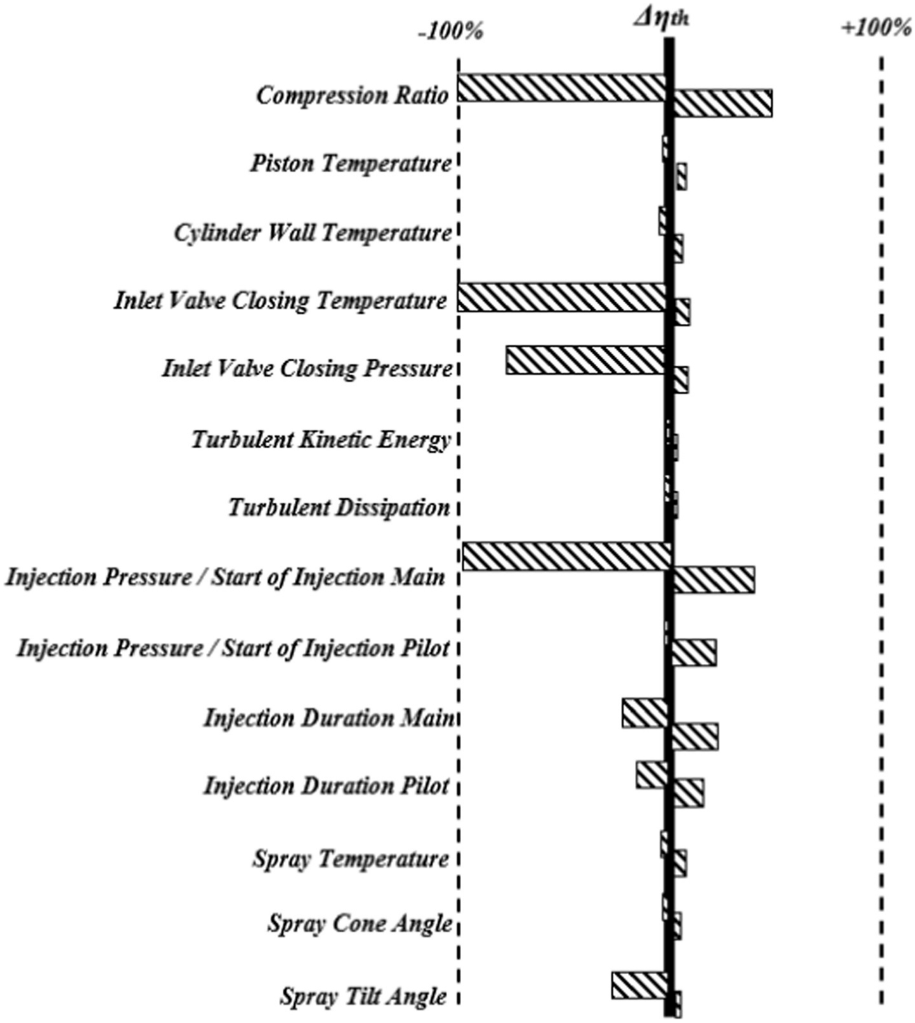

Fig. A2. Influence of the examined parameters on indicated thermal efficiency of the dual-fuel marine engine operating with 90 % MEF.

strategy emerged as exhibited considerable efficiency and low NOx emissions, without needing to increase the CR and T_{IVC}. The dual-fuel engine with optimised injection strategy reduces reliance on after-treatment systems for NOx emissions reduction, thereby facilitating simpler engine design and required control systems.

The parametric optimisation of methanol combustion in marine dual-fuel engines at low loads for the marine industry's transition to lower emissions and improved fuel efficiency. This study findings on the requited engine setting and in-cylinder phenomena addresses specific knowledge gaps for these engines operation at low loads yielding valuable insights to support the maritime industry's decarbonisation pathway.

While the study focused on a marine four-stroke large-bore engine, the findings can be transferred to other engine sizes and types, such as those used in rail or stationary power applications. The advantages from the use of stratified and multi-stage injection strategies can inform design improvements for engines of various scales, as they face similar challenges at low-load operation and the need for reduced emissions. Future research can evaluate specific modifications to adapt these strategies for smaller or larger engines with different combustion chamber geometries and operating envelopes.

The consideration of split injection strategies is associated with increased complexity of the injection system and its control. However, injectors durability may be compromised due to frequent high-pressure switching, which may also cause faster nozzle wear and erosion as well as carbon deposits. Additionally, for multiple injections can results in fuel spray interactions and wall impingement leading to incomplete combustion.

This study primarily investigates low-load conditions and does not cover the engine entire operational envelope. Furthermore, the engine operational challenges low loads must first be addressed, so that the engine can operate in higher loads. Additionally, optimisation was limited to specific CR and T_{IVC} parameters, and further refinement could explore more extensive parameter variations, including injection timing and EGR rates. Future studies could also address transient load conditions to understand how rapid shifts in power demand impact methanol combustion stability. Lastly, experimental validation in real-world marine engines would enhance confidence in the model's applicability and provide insights into other factors, such as fuel quality variability and ambient temperature effects on engine performance and emissions.

4. Conclusions

This study parametrically optimised the settings of a marine dual-fuel engine operating with 90 % methanol energy fraction. The investigation focused on low loads and considered several injection strategies (split and stratified). CFD models were developed for the considered marine engine. These CFD models were validated against experimental data for the considered engine operating in the diesel mode, whereas validation against reported experimental results for a light-duty methanol fuelled engine was also performed. The engine operation in 30 % load was investigated considering the same injector for both methanol and diesel fuels in different timings. Optimal values for compression ratio (CR) and temperature at inlet valve closing (TIVC) were selected for each injection strategy, the performance and emissions parameters of which were analysed. The study concluded in the following findings:

- High ranges of compression ratio and temperature at inlet valve closing are required, so that the unburnt methanol remains below the acceptable of 5 % for the single, two and three stage injection strategies. The engine operation in these conditions is challenging for marine dual fuel engines, which must facilitate operation in both the diesel and methanol modes.
- However, if these challenges are addressed at the design phase, the optimal selection for the single injection strategy (CR = 17 and T_{IVC} = 380 K) yields higher indicated thermal efficiency (53 %) compared to the optimal selections for the two and three stage injection strategies (50.4 % and 50.2 %, respectively). The estimated unburnt methanol (UM) emissions were 0.56 g/kWh (compared to 0.1, and 0.65 g/kWh respectively for the two- and three-stage injection strategies).
- The optimal selection for the two-stage injection strategy (CR = 17 and T_{IVC} = 360 K) yields the greater unburned methanol emissions 3.2 g/kWh.
- The optimal selection for the three-stage injection strategy exhibits high NOx emissions (12 g/kWh) significantly due to combustion duration increase.
- The stratified injection can be a solution to mitigate these challenges allowing for the engine operation at low ranges of compression ratio and temperature at inlet valve closing, exhibiting almost complete methanol combustion, associated with low NOx emissions (4.5 g/kWh) at the expense of lower indicated thermal efficiency compared with the other strategies.
- The engine operation at other loads exhibited similar behaviour with that identified for the 30 % load, deducing the validity of this study finding for the engine low load range.
- The stratified injection strategy is recommended for new designs of methanol fuelled marine dual fuel engines (operating with 90 % MEF).

This study provides valuable insights on the operating conditions of the methanol marine engine in low loads, hence supporting to the engine design decision-making and follow up optimisation studies. Future studies could deal with the methanol fuelled marine engine settings optimisation for each injection strategy and full operating envelope, as well as the design and control of the engine injection and turbocharging systems. In future work a 0D combustion model will be developed to investigate transient conditions.

CRediT authorship contribution statement

Panagiotis Karvounis: Writing – review & editing, Writing – original draft, Validation, Software, Methodology, Investigation, Formal analysis, Conceptualization. **Gerasimos Theotokatos:** Writing – review & editing, Supervision, Resources, Project administration, Methodology, Investigation, Formal analysis, Conceptualization. **Konstantinos Zoumpourlos:** Software, Resources. **Andrea Coraddu:** Supervision, Resources.

Declaration of competing interest

The authors declare that they have no known competing financial interests or personal relationships that could have appeared to influence the work reported in this paper.

Acknowledgements

The authors greatly acknowledge the funding from DNV AS and RCCL for the MSRC establishment and operation. The opinions expressed herein are those of the authors and should not be construed to reflect the views of DNV AS and RCCL. We would like to thank Convergent Science for offering their software (CONVERGE) and their technical support for the accomplishment of this research.

Appendix A

Table A1 introduces the CFD models characteristics including the reaction mechanism, combustion model, NOx mechanism, turbulence, droplet breakup and collision models, as well as wall heat transfer and spray sub-models.

Table A2 lists the validation of the CFD model results (maximum in-cylinder pressure, power output and NO emissions) against shop test measurements for the considered marine engine operation in the diesel mode. Table A3 lists the CFD model validation results for the engine operating in the gas mode with natural gas (and pilot diesel). Table A4 lists the injection parameters for the considered study including mass of methanol and diesel, injection duration and pressure of methanol and diesel.

Fig. A1 presents the results of the sensitivity study on turbulence energy and dissipation constants for the case of the stratified injection and optimal settings (CR = 14, TIVC = 360 K). Two extreme values are examined for turbulent kinetic energy (tke) and turbulent dissipation (td) ranging between –50 % and 200 % of their baseline values. Furthermore, the spray brake up constants are based on the authors' previous study investigating a marine engine with methanol and diesel direct injection [46]. The derived results demonstrate that the tke and td values only slightly affect the heat release, hence confirming the validity of the initial values for tke and td.

The sensitivity analysis is conducted with the aim to identify key parameters for the optimisation process. Table A5 includes 14 selected parameters that influence the performance of the marine engine. The analysis considers the dual-fuel operation with 90 % methanol energy fraction. According to Fig. A2 the most critical parameters to optimise are hierarchically, the compression ratio, inlet valve closing temperature and start of injection of main and pilot fuels. Other influencing parameters include the pressure at the inlet valve closing pressure, spray angles and injection duration. This study focused on CR and T_{IVC} for the optimisation process.

Data availability

No data was used for the research described in the article.

References

[1] S. Repka, A. Erkkilä-Välimäki, J.E. Jonson, M. Posch, J. Törrönen, J.P. Jalkanen, Assessing the costs and Environmental Benefits of IMO Regulations of Ship-Originated SOx and NOx Emissions in the Baltic Sea, Ambio 50 (9) (2019) 1718–1730.
[2] G. Theotokatos, P. Karvounis, G. Polychronidi, Environmental-economic analysis for decarbonising ferries fleets, Energies 16 (22) (2023 Nov 7) 7466.
[3] P. Karvounis, C. Tsoumpris, E. Boulougouris, G. Theotokatos, Recent advances in Sustainable and Safe Marine Engine operation with Alternative Fuels, Front. Mech, Eng, 2022.
[4] C.J. McKinlay, S.R. Turnock, D.A. Hudson, Route to Zero Emission Shipping: Hydrogen, Ammonia or Methanol? Int. J. Hydrogen Energy 46 (55) (2021).
[5] S. Verhelst, J.W.G. Turner, L. Sileghem, J. Vancoillie, Methanol as a fuel for Internal Combustion Engines, Prog. Energy Combust. Sci. 70 (2019) 43–88.
[6] Z. Tian, Y. Wang, X. Zhen, Z. Liu, The effect of Methanol Production and Application in Internal Combustion Engines on Emissions in the Context of Carbon Neutrality: a Review, Fuel 320 (2022) 123902.
[7] Public Final Report (MIIP001-2017.).
[8] K. Panda, A. Ramesh, Injection strategy of methanol for high loads and low NOx emissions in a neat methanol LTC engine, Int. J. Engine Res. 14680874231200525 (2023).
[9] L. Ning, Q. Duan, Z. Chen, H. Kou, B. Liu, B. Yang, K. Zeng, A Comparative Study on the Combustion and Emissions of a Non-Road Common Rail Diesel Engine Fuelled with Primary Alcohol Fuels (Methanol, Ethanol, and n-Butanol)/Diesel dual fuel, Fuel 266 (2020) 117034, https://doi.org/10.1016/j.fuel.2021.121360.

[10] A. Datta, B.K. Mandal, Impact of Alcohol Addition to Diesel on the Performance of Combustion and Emissions of a Compression Ignition Engine, Appl. Therm. Eng. 98 (2016) 670–682.
[11] J. Dierickx, Q. Dejaegere, J. Peeters, L. Sileghem, S. Verhelst, Performance and emissions of a high-speed marine dual-fuel engine operating with methanol-water blends as a fuel, Fuel 333 (2023) 126349.
[12] X. Yin, L. Xu, H. Duan, Y. Wang, X. Wang, K. Zeng, Y. Wang, In-depth comparison of methanol port and direct injection strategies in a methanol/diesel dual fuel engine, Fuel Process. Technol. 241 (2023) 107607.
[13] Y. Li, M. Jia, Y. Liu, M. Xie, Numerical Study on the Combustion and Emission Characteristics of a Methanol/Diesel Reactivity Controlled Compression Ignition (RCCI) engine, Appl. Energy 106 (2013) 184–197, https://doi.org/10.1016/j.apenergy.2013.01.058.
[14] Z. Li, Y. Wang, H. Geng, X. Zhen, M. Liu, S. Xu, C. Li, Parametric study of a diesel engine fueled with directly injected methanol and pilot diesel, Fuel 256 (2019) 115882.
[15] Zoumpourlos K, Coraddu A, Geertsma R, van de Ketterij R. Evaluation of Methanol Sprays in Marine Internal Combustion Engines: a Case Study for Port Fuel Injection Systems. Modelling and Optimisation of Ship Energy Systems 2023. 2023 Dec 24.
[16] B. Wang, A. Yao, C. Yao, C. Chen, H. Wang, In-Depth Comparison between Pure Diesel and Diesel Methanol dual fuel Combustion Mode, Appl. Energy 278 (2020) 115664, https://doi.org/10.1016/j.apenergy.2020.115664.
[17] S. Karimkashi, M. Gadalla, J. Kannan, B. Tekgül, O. Kaario, V. Vuorinen, Large-eddy simulation of diesel pilot spray ignition in lean methane-air and methanol-air mixtures at different ambient temperatures, Int. J. Engine Res. 24 (3) (2023) 965–981.
[18] P. Karvounis, G. Theotokatos, I. Vlaskos, A. Hatziapostolou, Methanol combustion characteristics in compression ignition engines: a critical review, Energies 16 (24) (2023 Dec 14) 8069.
[19] B. Gainey, J. Gandolfo, Z. Yan, B. Lawler, Mixing controlled compression ignition with methanol: an experimental study of injection and EGR strategy, Int. J. Engine Res. 24 (5) (2023) 1961–1972.
[20] Svensson, M., Tuner, M., & Verhelst, S. (2022). Low Load Ignitability of Methanol in a Heavy-Duty Compression Ignition Engine (No. 2022-01-1093). SAE Technical Paper.
[21] B. Wang, A. Yao, C. Chen, C. Yao, H. Wang, M. Liu, Z. Li, Strategy of improving fuel consumption and reducing emission at low load in a diesel methanol dual fuel engine, Fuel 254 (2019) 115660.
[22] B. Zincir, P. Shukla, S. Shamun, M. Tuner, C. Deniz, B. Johansson, Investigation of effects of intake temperature on low load limitations of methanol partially premixed combustion, Energy Fuel 33 (6) (2019) 5695–5709.
[23] H. Valera, D. Kumar, A.K. Agarwal, Evaluating the effect of variable methanol injection timings in a novel co-axial fuel injection system equipped locomotive engine, J. Clean. Prod. 349 (2022) 131452.
[24] D. Kumar, U. Sonawane, K. Chandra, A.K. Agarwal, Experimental investigations of methanol fumigation via port fuel injection in preheated intake air in a single cylinder dual-fuel diesel engine, Fuel 324 (2022) 124340.
[25] Y. Zhang, H. Wu, S. Mi, W. Zhao, Z. He, Y. Qian, X. Lu, Application of methanol and optimization of mixture design over the full operating map in an intelligent charge compression ignition (ICCI) engine, Fuel Process. Technol. 234 (2022) 107345.
[26] A. García, J. Monsalve-Serrano, C. Micó, M. Guzmán-Mendoza, Parametric evaluation of neat methanol combustion in a light-duty compression ignition engine, Fuel Process. Technol. 249 (2023) 107850.
[27] Z. Li, Y. Wang, Z. Yin, H. Geng, R. Zhu, X. Zhen, Effect of injection strategy on a diesel/methanol dual-fuel direct-injection engine, Appl. Therm. Eng. 5 (189) (2021 May) 116691.
[28] G. Huang, Z. Li, W. Zhao, Y. Zhang, J. Li, Z. He, X. Lu, Effects of fuel injection strategies on combustion and emissions of intelligent charge compression ignition (ICCI) mode fueled with methanol and biodiesel, Fuel 274 (2020) 117851.
[29] Y. Li, M. Jia, L. Xu, X.S. Bai, Multiple-objective optimization of methanol/diesel dual-fuel engine at low loads: a comparison of reactivity controlled compression ignition (RCCI) and direct dual fuel stratification (DDFS) strategies, Fuel 262 (2020) 116673.
[30] Pucilowski, M., Fatehi, H., Jangi, M., Lonn, S., Matamis, A., Andersson, O., ... & Bai, X. S. (2019). Numerical investigation of methanol ignition sequence in an optical PPC engine with multiple injection strategies (No. 2019-24-0007). SAE Technical Paper.
[31] M. Wen, C. Wang, Z. Zhang, Y. Wu, H. Liu, C. Jin, Z. Zheng, M. Yao, Effects of operating parameters on start performance of compression ignition engine by using high-pressure direct-injection pure methanol fuel, Appl. Therm. Eng. 15 (249) (2024 Jul) 123352.
[32] M. Jiang, W. Sun, L. Guo, H. Zhang, Z. Jia, Z. Qin, G. Zhu, C. Yu, J. Zhang, Numerical optimization of injector hole arrangement for marine methanol/diesel direct dual fuel stratification engines, Appl. Therm. Eng. 15 (257) (2024 Dec) 124456.
[33] L. Liu, Y. Wu, Y. Wang, J. Wu, S. Fu, Exploration of environmentally friendly marine power technology-ammonia/diesel stratified injection, J. Clean. Prod. 380 (2022) 135014.
[34] M. Jia, Y. Li, L. Xu, X.-S. Bai, Multiple-objective optimization of methanol/diesel dual-fuel engine at low loads: a comparison of reactivity controlled compression ignition (RCCI) and direct dual fuel stratification (DDFS) strategies, Fuel 262 (2020) 116673, https://doi.org/10.1016/j.fuel.2019.116673.
[35] G. Huang, Z. Li, W. Zhao, et al., Effects of fuel injection strategies on combustion and emissions of intelligent charge compression ignition (ICCI) mode fueled with methanol and biodiesel, Fuel 274 (2020) 117851, https://doi.org/10.1016/j.fuel.2020.117851.
[36] R.K. Maurya, A.K. Agarwal, Experimental investigations of performance, combustion and emission characteristics of ethanol and methanol fueled HCCI engine, Fuel Process. Technol. 1 (126) (2014 Oct) 30–48.
[37] P. Karvounis, G. Theotokatos, C. Patil, L. Xiang, Y. Ding, Parametric investigation of diesel–methanol dual fuel marine engines with port and direct injection, Fuel 381 (2025) 133441, https://doi.org/10.1016/j.fuel.2024.133441.
[38] Y.B. Zeldovich, The Oxidation of Nitrogen in Combustion explosions, Acta Physicochimica u.s.s.r. 21 (1946) 577–628.
[39] Fenimore CP. Formation of nitric oxide in premixed hydrocarbon flames. InSymposium (international) on combustion 1971 Jan 1 (Vol. 13, No. 1, pp. 373-380). Elsevier.
[40] F.S. Lien, E. Yee, Numerical modelling of the turbulent flow developing within and over a 3-d building array, part I: a high-resolution Reynolds-averaged Navier—Stokes approach, Bound.-Lay. Meteorol. 112 (2004) 427–466.
[41] L.M. Ricart, R.D. Reitz, J.E. Dec, Comparisons of diesel spray liquid penetration and vapor fuel distributions with in-cylinder optical measurements, J Eng Gas Turb Power 122 (4) (2000) 588–595.
[42] J.C. Andrae, R.A. Head, HCCI experiments with gasoline surrogate fuels modeled by a semidetailed chemical kinetic model, Combust. Flame 156 (4) (2009 Apr 1) 842–851.
[43] Y. Zhao, X. Liu, S. Kook, Effect of three-hole nozzle orientations on sprays and combustion in methanol-diesel dual direct injection engines, Appl. Therm. Eng. 1 (254) (2024 Oct) 123953.
[44] Bravo L, Kweon CB. A review on liquid spray models for diesel engine computational analysis. Army Research Laboratory Technical Report Series, ARL-TR-6932. 2014 May 1.
[45] Zoumpourlos, K., Geertsma, R., Ketterij, R. V. D., and Coraddu, A. (March 18, 2025). “Methanol Operation in Heavy-Duty DICI Dual-Fuel Engines: Investigating Charge Cooling Effects Using Engine Combustion Network Spray D Data.” ASME. *J. Eng. Gas Turbines Power*. October 2025; 147(10): 101007. https://doi.org/10.1115/1.4067862.
[46] K. Zoumpourlos, C. Bekdemir, R. Geertsma, R. van de Ketterij, A. Coraddu, CFD modeling approach for late-injection methanol sprays validated with ECN spray M, Int. J. Engine Res. 15 (2025 Mar) 14680874251323931.
[47] G. Kokkulunk, A. Parlak, H.H. Erdem, Determination of performance degradation of a marine diesel engine by using a curve-based approach, Appl. Therm. Eng. 108 (2016) 1136, https://doi.org/10.1016/j.applthermaleng.2016.08.019.
[48] R. Zang, C. Yao, Numerical study of combustion and emission characteristics of a diesel/methanol dual fuel (DMDF) engine, Energy Fuel 29 (6) (2015 Jun 18) 3963–3971.
[49] H. Hu, D. Lu, X. Zhang, H. Gan, Z. Huang, Study of EGR strategy for marine two-stroke methanol-diesel dual-fuel engines: Combustion, performance, and emission analysis across full operating range, Therm. Sci. Eng. Prog. 2 (2025 Sep) 104058.
[50] W. Sun, M. Jiang, L. Guo, H. Zhang, Z. Jia, Z. Qin, W. Zeng, S. Lin, G. Zhu, S. Ji, Y. Zhu, Numerical study of injection strategies for marine methanol/diesel direct dual fuel stratification engine, J. Clean. Prod. 1 (421) (2023 Oct) 138505.
[51] G. Papalambrou, V. Karystinos, Parametric Investigation of Methanol Ratio and Diesel Injection timing for a Marine Diesel–Methanol Dual-fuel Engine, Journal of Marine Science and Engineering. 13 (4) (2025 Mar 24) 648.
[52] B. Cao, Y. Yu, J. Yang, L. Hu, R. Jiang, B. Li, L. Xie, R. Zhang, Numerical analysis of the effect of fuel supply strategies on the combustion and emissions of a methanol/diesel dual-fuel marine low-speed engine, Pol. Marit. Res. (2025).
[53] P. Karvounis, G. Theotokatos, Parametric optimisation of diesel–methanol injection timings of a dual-fuel marine engine operating with high methanol fraction using CFD, Appl. Therm. Eng. 1 (264) (2025 Apr) 125433.
[54] P. Karvounis, G. Theotokatos, Performance improvement and emissions reduction of methanol fuelled marine dual-fuel engine with variable compression ratio, Fuel Process. Technol. 1 (272) (2025 Jul) 108208.
[55] M. Choi, S. Park, Optimization of multiple-stage fuel injection and optical analysis of the combustion process in a heavy-duty diesel engine, Fuel Process. Technol. 1 (228) (2022 Apr) 107137.
[56] J. Kannan, M. Gadalla, B. Tekgül, S. Karimkashi, O. Kaario, V. Vuorinen, Large-eddy simulation of tri-fuel ignition: diesel spray-assisted ignition of lean hydrogen–methane–air mixtures, Combust. Theor. Model. 25 (3) (2021 Apr 16) 436–459.
[57] Z. Li, Y. Wang, Y. Wang, Z. Yin, Z. Gao, Z. Ye, X. Zhen, Effects of fuel injection timings and methanol split ratio in M/D/M strategy on a diesel/methanol dual-fuel direct injection engine, Fuel 1 (325) (2022 Oct) 124970.
[58] A.O. Emiroglu, M. Sen, Combustion, Performance and Emission Characteristics of Various Alcohol Blends in a Single Cylinder Diesel Engine, Fuel 212 (2018) 34–40, https://doi.org/10.1016/j.fuel.2017.10.016.
[59] D. Kumar, H. Valera, A.K. Agarwal, Numerical predictions of In-Cylinder Phenomenon in Methanol Fueled Locomotive Engine using High pressure Direct Injection Technique, SAE Technical Paper (2021–01-0492, 2021.), https://doi.org/10.4271/2021-01-0492.
[60] M. Elkelawy, E.A. El Shenawy, S.A. Mohamed, M.M. Elarabi, H.A. Bastawissi, Impacts of EGR on RCCI engines management: a comprehensive review, Energy Convers. Manage.: X 1 (14) (2022 May) 100216.
[61] X. Yang, S. Gupta, T.W. Kuo, V. Gopalakrishnan, RANS and large eddy simulation of internal combustion engine flows—a comparative study, J. Eng. Gas Turbines Power 136 (5) (2014 May 1) 051507.
[62] M. Shi, B. Wu, J. Wang, S. Jin, T. Chen, Optimization of methanol/diesel dual-fuel engines at low load condition for heavy-duty vehicles to operated at high substitution ratio by using single-hole injector for direct injection of methanol, Appl. Therm. Eng. 1 (246) (2024 Jun) 122854.

[63] N. Nordin, Complex chemistry modeling of diesel spray combustion, Chalmers University, 2001. PhD thesis.
[64] Z.Y. Han, R.D. Reitz, A temperature wall function formulation for variable density turbulence flows with application to engines convective heat transfer modeling, Int. J. Heat Mass Transfer 40 (3) (1997) 613–625.
[65] P.J. O`Rourke, A.A. Amsden, The TAB Method for Numerical Calculation of Spray Droplet Breakup. SAE Technical Paper 872089, Society of Automotive Engineers (1987).